NTNU – Trondheim
Norwegian University of
Science and Technology

Non-linear Analysis of Wind Load Subjected Novel Flare Tower Design for Sevan Marine

Jon Eirik Knutsen Nøding

Marine Technology
Submission date: June 2012
Supervisor: Bernt Johan Leira, IMT

Norwegian University of Science and Technology
Department of Marine Technology

NTNU
Norwegian University of Science and Technology
Department of Marine Technology

Master thesis, Spring 2012
for
Stud. Techn. Jon Eirik Nøding

Analysis and Design of Flare Tower Subjected to Wind Loading

Analyse og Dimensjonering av Flammetårn Utsatt for Vind-belastning

A new structural concept for a flare tower located on an offshore platform is to be designed and analysed. The static and dynamic loads on such a tower will also need to be re-considered due to the novelty of the structural layout. Based on information received from Sevan Marine, the candidate will perform an assessment of the proposed concept. Numerical response analysis is to be performed by means of the computer program Abaqus. Algorithms for evaluation of the wind loading are to be developed by the candidate. If it is found to be required (e.g. for estimation of VIV frequencies), the candidate can establish simplified analysis tools e.g. by application of Excel or Matlab.

The following subjects are to be examined in this thesis:

1. Give a general description of typical designs of existing flare towers and the loads that need to be taken into account. Discuss which design guidelines that are relevant for these types of structures.

2. The previous Finite Element model of the Sevan flare boom in Genie is to be remade into a corresponding model in Abaqus for the purpose of parametric studies with respect to structural layout. A wind load simulation algorithm is to be implemented in Abaqus for the case of first order wind load effects.

3. Parametric studies are to be performed for a base case structural model with respect to the type of response analysis (i.e. linear versus nonlinear, quasistatic versus dynamic) and with respect to convergence of the mesh refinement. A matrix of cases to be analysed is to be agreed upon with the supervisor prior to start of the analyses themselves.

4. The main principles behind a VIV type of response analysis are to be briefly explained. Design consideration to be made in order to avoid significant response levels for this type of response (e.g. adjustment of natural frequencies or application of helical strakes) are to be discussed.

5. Analysis of the structure with respect to the fracture/fatigue limit state is to be performed in addition to the ultimate limit state (ULS).

6. Optimization of the tower structure (e.g. based on minimum weight criteria) is to be investigated to the extent that time allows.

The work-scope may prove to be larger than initially anticipated. Subject to approval from the supervisor, topics may be deleted from the list above or reduced in extent.

In the thesis the candidate shall present his personal contribution to the resolution of problems within the scope of the thesis work. Theories and conclusions should be based on mathematical derivations and/or logic reasoning identifying the various steps in the deduction. The candidate should utilise the existing possibilities for obtaining relevant literature.

The thesis should be organised in a rational manner to give a clear exposition of results, assessments, and conclusions. The text should be brief and to the point, with a clear language. Telegraphic language should be avoided.

The thesis shall contain the following elements: A text defining the scope, preface, list of contents, summary, main body of thesis, conclusions with recommendations for further work, list of symbols and acronyms, references and (optional) appendices. All figures, tables and equations shall be numerated.

The supervisor may require that the candidate, at an early stage of the work, presents a written plan for the completion of the work. The plan should include a budget for the use of computer and laboratory resources which will be charged to the department. Overruns shall be reported to the supervisor.

The original contribution of the candidate and material taken from other sources shall be clearly defined. Work from other sources shall be properly referenced using an acknowledged referencing system.

The thesis shall be submitted in 3 copies:

- Signed by the candidate
- The text defining the scope included
- In bound volume(s)
- Drawings and/or computer prints which cannot be bound should be organised in a separate folder.

Supervisor: Professor Bernt J. Leira Contact person at Sevan:

Start: January 16th, 2012 Deadline: June 14th, 2012

Trondheim, 16th January 2012

Bernt J. Leira

Scope

This master thesis is a a case study of a novel flare tower design, proposed by Sevan Marine. It is a continuation of a specialization project, concerning the same subject. The design in consideration is in relation to the Sevan 400 cylindrical FPSO.

The thesis describes the computational design of the proposed structure using the preprocessor Patran Pre. It also describes the loads the structure is subjected to, with main focus on wind loads, how they are calculated and modeled in the software. Different load cases have been applied to the tower, using the FEM software Abaqus. The types of analysis conducted are quasi-static wind load, dynamic wind load, plastic analysis and buckling. Platform motions have been included as supplied by Sevan Marine. Mesh refinement have been performed to check for convergence and other mesh size dependent effects. The report includes discussions of the results and recommendations for design changes and further work.

In addition to the numerical calculations an outline of existing flare tower designs have been given, including the relevant guidelines for these structures. It also describes VIV, its effect on the structure and how it might be counteracted.

Preface

This thesis is a part of the master program at the Institute of Marine Technology, NTNU. The design to be analyzed where presented by Kåre Syvertsen at Sevan Marine ASA, a supplier to the international offshore oil and gas industry. He has supplied the necessary input information for the thesis, and helped to specify the task. Professor Bernt J. Leira, at the Institute of Marine Technology, has been the thesis supervisor. He has defined the subjects to be examined, supplied relevant literature when needed and generally been of great help and assistance during the process.

In working with the Patran Pre software both Martin Storheim, PhD at Institute of Marin Technology and Frank Klæbo at Sintef Marintek have been of great assistance. Frank Klæbo has also assisted with implementing the Patran Pre output into the Abaqus FEM software.

I would also like to thank Morten Sletteberg Haugen for help with procrastination by the pool table...

Summary

This paper show that the novel flare tower design presented by Sevan Marine has potential. Numerical calculations show that the dimensions of the tower are appropriate. Some design changes should be considered. There are aspects related to the dimensioning that are yet to be analyzed.

In this paper, a novel flare tower design has been designed and analyzed. Relevant regulations and offshore loads have been examined and implemented. The purpose of this was to consider wether the design would be usable as an alternative to the traditional flare tower designs. The questions to be answered were:

- What loads are the structure subjected to in an ULS consideration.
- What kind of dynamics would the tower be subjected to.
- Is the tower design strong enough to withstand these loads.
- Could the design be a real alternative to traditional flare towers.
- Could the design be superior to traditional flare towers.

Quasi-static wind load and wind specter load were applied to the tower, in addition to platform motions. Load responses were found using Abaqus and Matlab. The tower was found to have dynamic responses due to the wind specter load and vortex induced vibrations. The tower design appear to be sufficiently strong, assuming some design modifications like removal of cut outs or stiffening. This paper show that the novel flare tower design is a worthy competitor to the traditional flare tower designs. It might even be superior.

The major implications from this is that the design could replace older and outdated designs, giving a cheaper, less complex structure that would be safer and easier to maintain.

Contents

List of Tables

List of Figures

Symbols and Abbreviations

Constants

$g = 9,81 m/s^2$ - Acceleration of gravity

$E = 2,1 \cdot 10^{11} Pa$ - Young´s modulus of steel

$\nu_{air} = 1,529 \cdot 10^{-5} m^2/s$ - Kinematic viscosity of air

$\nu = 0,3$ - Poisson´s ratio of steel

$\rho_{air} = 1,25 kg/m^3$ - Air density

$\rho_{steel} = 7,85 \cdot 10^3 kg/m^3$ - Steel density

Symbols

B^2 - Background factor

c_{dir} - Directional factor

C_D - Drag coefficient

C_D^s - Drag coefficient factor

c_{season} - Seasonal factor

c_f - Force factor

$c_{f,0}$ - Force factor without free-end flow

c_r - Roughness factor

c_O - Orography factor

$C_s C_d$ - Construction factor

D(h) - Height dependent diamter

f_L - Non-dimensional frequency

f - Non-dimensional frequency

f_n - Eigenfrequency

f_v - Vortex shedding frequency

h - Height

I_v - Turbulence intensity

k - Equivalent surface roughness

k_{10} - Surface roughness parameter

k_I - Turbulence factor

k_p - Peak factor

k_r - Terrain roughness factor

L_t - Reference length scale

m_i - Spectral moment i

n - Frequency

n_τ - Number of global maxima

n_i - Eigenfrequency of the structure

q_p - Peak velocity pressure

q_t - Frequency dependent wind pressure

R^2 - Resonance response factor

Re - Reynolds number

R_b - Aerodynamic admittance function

R_h - Aerodynamic admittance function

S_L - Non-dimensional power spectral density function

$S_{\dot{u}}$ - Kaimal wind speed specter

S_{MPa^2} - Response specter

t - Shell thickness

t_0 - Zero-up-crossing period

T - Averaging time for the mean wind velocity

$\overline{U}$ - Middle wind speed

$\overline{U_{10}}$ - Middle wind speed at 10m height

U_R - Reduced velocity

$\dot{u}$ - Turbulent wind speed

$u_\star$ - Wind shear velocity

v - Peak wind velocity

v_b - Basic wind speed

$v_{b,0}$ - Reference wind speed

v_m - Middle wind speed

X_{max} - Expected largest value

z_0 - Roughness length

z_e - Reference height

z_r - Reference height

z_s - Reference height

z_t - Reference height

z_{min} - Minimum height

z_{max} - Maximal height

α - Surface roughness factor

α_1 - Mass damping

α_2 - Stiffness damping

δ - Total logarithmic damping decrement

δ_s - Logarithmic decrement of structural damping

δ_a - Logarithmic decrement of aerodynamic damping

δ_d - Logarithmic damping due to special devices.

Δ - Change in diameter per meter height

Δn - Frequency increments

γ_M - Material safety factor

ϕ_λ - End-effect factor

λ -

μ - Mass per unit area of structure

μ_e - Equivalent mass per unit area of structure

η_b - Aerodynamic factor

η_h - Aerodynamic factor

ν - Up-crossing frequency

Φ - Mode shape

σ - Variance

σ_v - Standard deviation

σ_Y - Yield strength

τ - Load duration

ζ - Mode shape factor

Abbreviations

ULS - Ultimate Limit State

ALS - Accidental Limit State

VIV - Vortex Induced Vibrations

MDS - Material Data Sheet

CFD - Computational Fluid Dynamics

NA - National Annex

FPSO - Floating production storage and offloading platform

FEM - Finite element method

FEA - Finite element analysis

Chapter 1

Flare tower design

1.1 Typical flare tower designs

For a typical flare boom design on an offshore installation a truss work concept is used. This is traditionally considered [10] a very effective strength to weight design, which is important on offshore platforms that are generally highly weight sensitive. In truss works it is also easy to calculate the tensions in the structure in a very reliable manner. This has been very important in pre-computer eras and results in effective use of engineering hours for each structure.

It is on the other hand quite labour intensive to build flare towers this way. A lot of welding is needed and the quality of the joint welds is very important to the end result. This means that they are relatively expensive to build and check for construction flaws. The large number of joints give many areas where tension can build locally, and dynamics make them vulnerable to fatigue. The dimensions, complexity and difficult working conditions they represent also make accessibility and maintenance difficult and expensive. Personnel with mountain climbing equipment and sufficient training is needed for the simplest tasks.

Flare towers are affected by different loads. Gravity and platform accelerations result in loads due to the weight of the tower, piping, flare pack and such. These are relatively easy to predict and design for. Wind loads on the other hand are much more difficult to predict. This is especially true on a a truss work structure. This is because different effects like Vortex Induced Vibrations (VIV), damping and wake effects are complicated to predict. They also give results that are highly uncertain. These effects, combined with stress concentrations give vibrations and fatigue problems.

1.2 Relevant guidelines

Since a flare tower is part of a larger offshore structure it is governed by a set of design rules [1, (2)]. One of the most basic of these are the NORSOK standards. The N-001 for general use, N-003 for load predictions, N-004 for the steel structure design and the M-120 for material choice are important. These also refer to other offshore standards like the DNV OS-C101, the ISO 19 900 series, the onshore standards NS 1991-1-4 and NS 3472 and the german DIN 4131 and 4133 to be used as supplements. Together they form a robust framework for designing and constructing an offshore structure like a flare tower. Many of these have been used in the design of the project flare tower. They are in turn a part of the larger national Health, Safety and Environment regulation hierarchy.

1.3 Advantages of novel flare tower design

When a largely different flare tower design is suggested it is due to certain assumptions related to the superiority of the alternative design:

- A simpler construction will result in a faster and less expensive production
- Reduction of weight due to better strength optimization
- Wind protection of the flare piping
- Reduced fatigue problems due to fewer stress concentration points
- Increased accessibility and safer working environment when performing maintenance
- Removed "lock-in" problem since increased diameter decreases reduced velocity
- Removal of wake effect problems

The "helix" is included to decrease VIV and to provide ventilation in case of a gas leakage within the tower.

Given that these assumptions prove true the alternative flare tower design will be far superior to the traditional flare tower in terms of cost, production time, fatigue problems and maintenance.

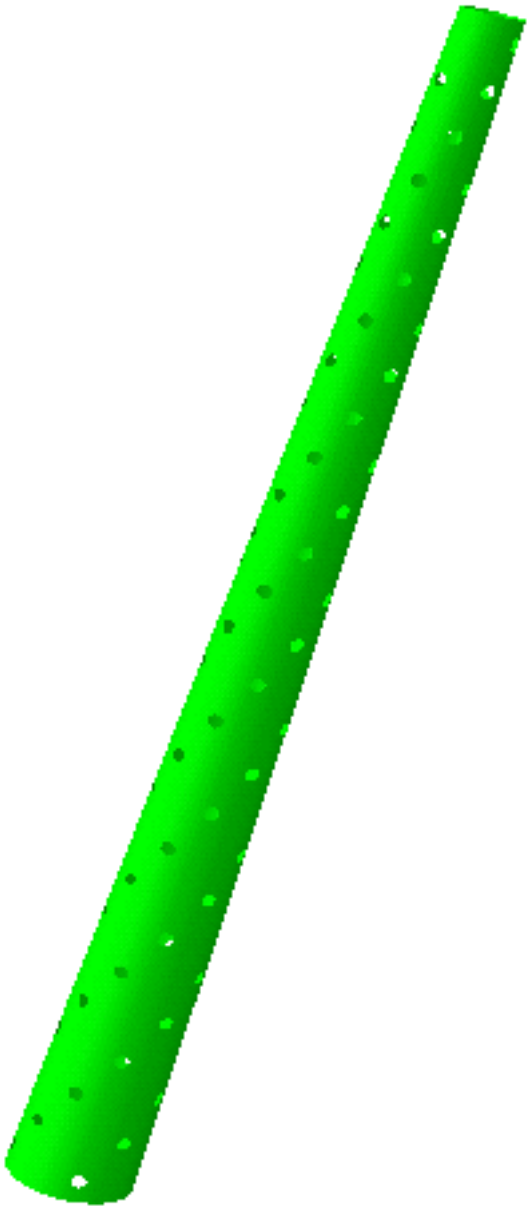

Figure 1.1: Flare tower model

Chapter 2

Structure

2.1 General

In general the flare tower consists of a cylindrical pipe made from thin metal plates, comprising a shell. It has a linearly varying size with the largest diameter at the bottom, where strength is important. The shell thickness is homogenous throughout the tower, but a possible variation of thickness could be considered.

In addition to the shell there is a flare pack at the top for burning off excess gas during drilling or production. Leading from the platform to the flare pack are piping, attached to the inside of the tower. A ladder is installed along the piping, for convenient access to the pipes, flare pack and the tower i general, making control and maintenance tasks easy, and relatively safe.

In spiraling "helix" patterns a large number of circular cutouts are made in the shell, from top to bottom. These will, theoretically, reduce the vortex induced vibration of the tower, similarly to external helical strakes on onshore smoke stacks and similar. They will also reduce the danger of accumulated leaked gas by providing ventilation.

Initially there will be no stiffening of the tower, as it is assumed that the shell itself will be strong enough to sustain the different types of loading the tower will be subjected to. Both longitudinal and circumferential stiffeners might be considered if it proves necessary.

2.2 Dimensions

The dimensions of the tower have been supplied by Sevan marine [16]. The base of the tower will be placed on the deck of a Sevan FPSO at height 16m above sea level. The height of the tower is 54m and it will be tilted at an angle of 15° from the vertical line, outwards. The diameter at the base is 5m, linearly decreasing to 2,3m at the top. The initial shell plate thickness is 10mm. The ventilation cutouts have a diameter of 0,6m, and are spaced approximately 1,8m apart. There are four parallel helixes.

2.3 Material properties

An appropriate material quality was used, acquired from the NORSOK standards [3, (5.2)]. When considering different types of materials, certain assumptions were made. It was assumed that failure of the structure would have no substantial consequences, as defined in NORSOK. The reason for this is that a failure in the tower most likely would occur during harsh weather conditions. In such circumstances there would be no hydrocarbon production, nor any staff in the tower. It would also collapse outwards, away from the platform deck. A total collapse could damage the platform, but to a small degree. This combined with no structural joints, a material design class DC4 is satisfactory, requiring a steel quality of level III. According to MDS - Y05 for "Plates and sections" a material grade of S355J0 with $\sigma_Y = 355$ MPa can be chosen [4] for the flare tower.

As steel is not always homogenous and might have undetected material flaws that can affect its strength, a safety factor must be applied. According to the standards [1, (7.2.3)] a materials safety factor of $\gamma_M = 1{,}15$ is sufficient. A yield strength of $\sigma_Y = \frac{355}{1{,}15} = 309$ MPa was used as material limit.

The steel used was assumed to have linear elastic properties with Young´s modulus of E $= 2,05 \cdot 10^5$ Gpa, Poisson´s ratio of 0,3 and plastic behavior above 309 MPa. A material density of $\rho_{steel} = 7,85 \cdot 10^3 kg/m^3$ was used.

2.4 Structural mass

For some load considerations, the structural mass was important to know, prior to the FE analysis. The total shell area of the flare tower is $\frac{2,3+5}{2}\pi \cdot 54 = 620m^2$. With an initial shell thickness of 0,01m and material density of $7,85 \cdot 10^3$ the structural

mass of the tower is $48,6 \cdot 10^3 kg$. The reduction of mass due to the cutouts are $(\frac{0,6}{2})^2 \pi \cdot 4 \cdot 27 \cdot 0,01 \cdot 7850 = 2,4 \cdot 10^3 kg$. This gives a resulting structural mass of 46,2 tons. According to information supplied by Sevan marine [16], the mass of the flare pack is 2,5 tons and piping and ladder is 8 tons combined. This gives a total mass of the flare tower of 56,7 tons.

2.5 Boundary conditions

The flare tower is welded to the platform. The strength of this connection is assumed to be sufficient to prevent any translational or rotational movement. The boundary conditions have been modeled as fixed for both translations and rotations, in all degrees of freedom, for the connection. The top end of the tower is on the other hand not connected to anything and it is consequently assumed that all degrees of freedom for both translations and rotations are free.

Chapter 3

Loads

3.1 General

The loads included in this analysis are either permanent loads, or environmental loads. Permanent loads include the weight of the structure, flare pack, piping and ladder. Environmental loads include accelerations from platform movement and wind loads. The weight has been multiplied with corresponding accelerations to find the different load vales.

When checking whether the structure is sufficiently strong for the ULS condition, the standards require that the loads be checked for different action combinations. The safety factors related to these action combinations are as shown in table 3.1 [1, (6.2.1)]

Action combinations	Permanent actions	Variable actions	Environmental actions
a	1.3	1.3	0.7
b	1.0	1.0	1.3

Table 3.1: Action Combinations

The worst combination is to be chosen.

3.2 Permanent loads

The permanent loads consists of forces on the structure, independent of weather conditions and temporary equipment. In the case of the flare tower, these are due

to the masses related to the tower as described in section 2.4. These masses are affected by the gravitational acceleration g, resulting in loads.

The value of these loads are:

	Mass [kg]	Load [kN]
Structure	46200	453,2
Flare pack	2500	24,5
Piping and ladder	8000	78,5
Sum	56700	556,2

Table 3.2: Permanent Loads

3.3 Platform movement

As the platform operates in harsh weather conditions, the waves and wind will cause significant motion. The accelerations related to these motions also affect the flare tower, as it is rigidly connected to the platform. To be in accordance with the standards, accelerations caused by a sea state with annual return period of 10^{-2}, per year, need to be accounted for [2, (6.1.1)].

The platform motions to be used have been calculated for the relevant platform and sea state by Sevan Marine [16]. From these results, the accelerations have been found by interpretation of the RAO curves showed in appendix C.1 and C.2.

	H_S [m]	T_P [s]	acc./H_S	acc. [m/s^2]
Horizontal acceleration	14.4	15.1	0.089	1.28
Vertical acceleration	13.0	11.5	0.138	1.80

Table 3.3: Platform accelerations

From the information sent by Sevan marine it was assumed that the motion results for the helideck and process deck stern are appropriate for the horizontal and vertical accelerations, respectively.

These accelerations give the following loads:

	Weight [kg]	Load x-dir [kN]	Load z-dir [kN]
Structure	46200	59,1	83,2
Flare pack	2500	3,2	4,5
Piping and ladder	8000	10,2	14,4
Sum	56700	72,6	102,0

Table 3.4: Platform acceleration loads

As no values for the rotational degrees of freedom were supplied they have not been included.

3.4 Wind loads

The main environmental load on the flare tower is due to wind. At large heights the wind can be quite strong, resulting in significant loads to the structure. Wind, being a dynamic load, will induce dynamic response in the structure. These dynamic loads can, especially if the wind frequencies are in the vicinity of the structural eigenfrequency, result in large responses. This can be damaging in terms of possible failures of the structure, but is also important in regards to fatigue. Wind loads are in addition highly unpredictable.

A particular phenomenon related to wind affected towers are Vortex Induced Vibrations (VIV). This is response in the structure created by vortices in the wake of the tower that can be highly problematic if not accounted for. The topic will be discussed in chapter 8.

Two different approaches have been used when calculating the wind load. One, using procedures from the Eurocode standard [5], outlined in chapter 4, and calculated using the Matlab script presented in appendix A.3. The other, using wind specter analysis, outlined in section 5, and calculated using the Matlab script presented in appendix A.4.

The first wind load procedure, acquired from the Eurocode was used to find the forces needed in the load combination consideration. A peak pressure of 2068 Pa were calculated. Multiplied with the surface area facing the wind direction, $\frac{2.3+5}{2} \cdot \pi \cdot 54 = 309,6m^2$, the resulting wind force were found to be 640 kN.

3.5 Load combinations

As stated in the standards [1, (6.2.1)], the worst load combination has to be chosen as the design load. From table 3.5, the loads, with safety factors, are given in the relevant directions.

	Permanent actions		Environmental actions		Sum		
	x-dir	z-dir	x-dir	z-dir	x-dir	z-dir	$\sqrt{x^2+z^2}$
a	0	723,0	498,8	71,4	498,8	794,4	938,0
b	0	556,2	926,4	132,6	926,4	688,8	1154,4

Table 3.5: Load combinations

This shows that load combination "b" give the largest loads on the structure. In the Abaqus analysis the accelerations and wind pressure were used. Combination "b" gave input as described in table 3.6

	Permanent actions			Environmental actions					
	Factor	Original	Result	Factor	Original	Result	Factor	Original	Result
X	1,0	0	0	1,3	1,28	1,66	1,3	2068	2688
Z	1,0	9,81	9,81	1,3	1,8	2,34	1,3	0	0

Table 3.6: Resulting actions

Chapter 4

Wind load approximation

The Eurocode 1991-1-4 is a standard primarily written for onshore structures. It is applicable for offshore structures, with the "National Annex" (NA) included, as emphasized in the national foreword. It gives a method that is load frequency independent. Dynamic aspects like wind turbulence, structural vibrations, factors related to shape and friction, pressure correlation and damping are taken into account, but as approximations. 10^{-2} annual probability wind load values are produced. The method is suitable for quasi-static analysis, but unsuitable for dynamic analysis.

4.1 Wind Calculations

The wind force on the structure is given as:

$$F_w = C_s C_d \cdot c_f \cdot q_p(z_e) \cdot A_{ref} \tag{4.1}$$

Where $C_s C_d$ is the construction factor [5, p.28], c_f is the force factor [5, p.71], q_p is the peak velocity pressure [5, p.22] at reference height z_e and A_{ref} is the reference area that is affected by the wind.

In regards to z_e; it is according to the Eurocode [5, p.71] defined as the largest height for the relevant cross section. Since the cross section in this case is varying, a height of $\frac{2}{3} \cdot$ tower height + deck height $= \frac{2}{3} \cdot 54 + 16 = 52m$ is chosen. This was considered a satisfying approximation.

4.2 Peak velocity pressure - q_p

$$q_p(z) = [1 + 7 \cdot I_v(z)] \cdot \frac{1}{2} \cdot \rho_{air} \cdot v_m^2(z) \tag{4.2}$$

Where I_v is the turbulence intensity [5, p.22], ρ_{air} is the air density and v_m is the middle wind speed [5, p.19].

$$v_m(z) = c_r(z) \cdot c_0(z) \cdot v_b \tag{4.3}$$

Where c_r is the roughness factor[5, p.19], v_b is the basic wind speed [5, p.18] and c_0 the orography factor taken as 1,0, since no alterations for "flat terrain" is required in the NA.

$$c_r(z) = k_r \cdot ln\left(\frac{z}{z_0}\right) \qquad \text{for} \qquad z_{min} \leq z \leq z_{max} \tag{4.4}$$

$$c_r(z) = c_r(z_{min}) \qquad \text{for} \qquad z \leq z_{min} \tag{4.5}$$

Where $k_r = 0,16$, $z_0 = 0,003m$, $z_{min} = 2m$ [5, NA Table 4.1] and $z_{max} = 200m$ [5, p.20].

$$v_b = c_{dir} \cdot c_{season} \cdot v_{b,0} \tag{4.6}$$

Where v_b is the basic wind speed at 10m elevation and terrain category II, $c_{dir} = 1,0$, is the directional factor, $c_{season} = 1,0$, is the season factor and $v_{b,0} = 32 \cdot 1.34 = 43m/s$ is the reference wind speed, as defined in figure NA.4(901.1) [5, NA p.8]. c_{dir} and c_{season} were given as 1,0 since the structure can be affected from all directions and for all seasons.

$$I_v(z) = \frac{\sigma_v}{v_m(z)} \qquad \text{for} \qquad z_{min} \leq z \leq z_{max} \tag{4.7}$$

$$I_v(z) = I_v(z_{min}) \qquad \text{for} \qquad z \leq z_{min} \tag{4.8}$$

Where $\sigma_v = k_r \cdot v_b \cdot k_I$. Here, $k_I = 1,0$, as no alterations for "flat terrain" is required in the NA.

4.3 Construction factor - C_sC_d

In the case of circular cylinders, C_sC_d can be assumed equal to 1.0, given that the height of the cylinder is less than 60 m and less than 6.5·$diameter$. When including the height of the platform, the flair boom is neither, and must be calculated using the [5, (6.3.1)] section.

$$C_sC_d = \frac{1 + 2 \cdot k_p \cdot I_v(z_s) \cdot \sqrt{B^2 + R^2}}{1 + 7 \cdot I_v(z_s)} \tag{4.9}$$

Where k_p is the peak factor, B^2 is the background factor, R^2 is the resonance response factor and $z_s = 0.6 \cdot h + 16 = 48m$ [5, Figure 6.1], is the reference height for determining the structural factor. k_p, B^2 and R^2 can, according to the NA be found using appendix B in the Eurocode [5, p.102]

$$k_p = \sqrt{2 \cdot ln(\nu \cdot T)} + \frac{0,6}{\sqrt{2 \cdot ln(\nu \cdot T)}} \text{ or } k_p = 3 \text{ ,depending of which is largest} \tag{4.10}$$

Where ν is the up-crossing frequency and T=600s is the averaging time for the mean wind velocity [5, p.104].

$$\nu = n_{1,x}\sqrt{\frac{R^2}{B^2 + R^2}} \quad ; \quad \nu \leq 0,08\text{Hz} \tag{4.11}$$

Where $n_{1,x}$ is the first eigenfrequency of the structure in the x-direction.

$$B^2 = \frac{1}{1 + 0,9 \cdot \left(\frac{b+h}{L(z_s)}\right)^{0,63}} \tag{4.12}$$

Where b and h is the width and height of the structure and $L(z_s)$ is the turbulent length scale.

$$L(z) = L_t \cdot \left(\frac{z}{z_t}\right)^{\alpha} \qquad \text{for} \qquad z \leq z_{min} \tag{4.13}$$

$$L(z) = L(z_{min}) \qquad \text{for} \qquad z \geq z_{min} \tag{4.14}$$

Where $z_t = 200m$ is a reference height and $L_t = 300m$ is a reference length scale [5, p.102] and $\alpha = 0,67 + 0,05ln(z_0)$.

$$R^2 = \frac{\pi^2}{2 \cdot \delta} \cdot S_L(z_s, n_{1,x}) \cdot R_h(\eta_h) R_b(\eta_b) \tag{4.15}$$

Where δ is the total logarithmic decrement of damping [5, p.143], S_L is a non-dimensional power spectral density function and R_h and R_b are aerodynamic admittance functions.

$$S_L(z, n) = \frac{6,8 \cdot f_L(z, n)}{1 + 10,2 \cdot f_L(z, n))^{5/3}} \tag{4.16}$$

Where $f_L(z, n) = \frac{n \cdot L_(z)}{v_m(z)}$,is a non-dimensional frequency, n being the eigenfrequency of the structure.

$$R_h = \frac{1}{\eta_h} - \frac{1}{2 \cdot \eta_h^2}(1 - e^{-2 \cdot \eta_h}) \tag{4.17}$$

$$R_b = \frac{1}{\eta_b} - \frac{1}{2 \cdot \eta_b^2}(1 - e^{-2 \cdot \eta_b}) \tag{4.18}$$

Where $\eta_h = \frac{4,6 \cdot h}{L_(z_s)} \cdot f_L(z_s, n_{1,x})$ and $\eta_b = \frac{4,6 \cdot b}{L_(z_s)} \cdot f_L(z_s, n_{1,x})$

$$\delta = \delta_s + \delta_a + \delta_d \tag{4.19}$$

Where δ_s is the logarithmic decrement of structural damping, δ_a is the logarithmic decrement of aerodynamic damping and δ_d is the logarithmic damping due to special devices. $\delta_s = 0,012$ from table F.5 in the eurocode for "Unlined welded

steel stacks without external thermal insulation" and $\delta_d = 1,0$, as there are no special damping devices involved.

$$\delta_a = \frac{c_f \cdot \rho_{air} \cdot v_m(z_s)}{2 \cdot n_{1,x} \cdot \mu_e} \tag{4.20}$$

Where c_f is the force factor described in section 4.4 and μ_e is the equivalent mass per unit area of the structure.

$$\mu_e = \frac{\int_0^h \int_0^b \mu(y,z) \cdot \Phi^2(y,z) dydz}{\int_0^h \int_0^b \Phi^2(y,z) dydz} \tag{4.21}$$

Where μ(y,z) is the mass per unit area of the structure and Φ(y,z) is the mode shape [5, p.127]. The structure is symmetrical about the z-axis, and thus independent of the y-variable.

$$\mu(z) = \pi \cdot (d - \Delta \cdot z) \cdot t \cdot \rho_{steel} \tag{4.22}$$

$$\Phi^2(z) = \left(\frac{z}{h}\right)^{2\zeta} \tag{4.23}$$

Where d = 5m, is the bottom diameter, $\Delta = 0,05$, is the change in diameter per meter height, t is the shell thickness, ρ_{steel} is the material density of steel and $\zeta = 2$.

4.4 Force factor - c_f

$$c_f = c_{f,0} \cdot \phi_\lambda \tag{4.24}$$

Where $c_{f,0}$ is the force factor for cylinders without free-end flow, and ϕ_λ is end-effect factor.

$$c_{f,0} = \frac{0,11}{(Re/10^6)^{1,4}} \qquad \text{, for Re} \lesssim 10^4 \tag{4.25}$$

$$c_{f,0} = 1,2 + \frac{0,18 \cdot log(10 \cdot k/b)}{1 + 0,4 \cdot log(Re/10^6)} \qquad \text{, for Re} \gtrsim 10^4 \tag{4.26}$$

Where Re is the Reynolds number and k is the equivalent surface roughness of the structure. The value for k can be found from table 7.13 in the Eurocode [5, p.64]. For a surface treated with spray paint k is $2 \cdot 10^{-5} m$.

$$Re = \frac{b \cdot v(z_e)}{\nu_{air}} \tag{4.27}$$

Where b is the width of the structure, ν_{air} is the kinematic viscosity of air and $v(z_e)$ is the peak wind velocity at height z_e.

$$v(z_e) = \sqrt{\frac{2 \cdot q_p(z_e)}{\rho_{air}}} \tag{4.28}$$

The end-effect factor can be found from figure 7.36 and table 7.16 in the Eurocode [5, p.71-72]. In the case of structural heights larger than 50m, $\lambda = 0,7 \cdot l/b$, or $\lambda = 70$, dependent on which is the smallest. Using $b = \frac{5+2,3}{2} = 3,65$ his results in $\lambda \approx 10$. Choosing the solidity ratio as $\approx 1,0$ results in $\phi_\lambda = 0,7$.

Chapter 5

Wind specter analysis

5.1 Theoretical background

A more precise method of calculating the wind load on the flare tower, than the one used in the Eurocode, utilizes wind specters. For structures that are sensitive to wind loads, like flare towers, a dynamic response analysis should be performed. The dynamic load is described by the wind specter [12, 3.5].

The wind energy depends on the frequency, and a wind specter represents this variation of energy. The wind velocity can be idealized as a superposition of a stochastic high frequency gust velocity and a slowly varying mean wind, which carries the bulk of the energy. When high frequencies are considered the dynamics of the structure will be induced by the gust velocity. The gust wind speed can be modeled using a Kaimal wind specter, described in equation 5.5, and will be considered a harmonic load.

Dynamic wind energy, in the eigenfrequency region, will cause large dynamic response. Even if the energy decreases in the high-frequency parts of the specter, it might still be enough to result in large excitations. The stress response related to these excitations can be found by creating a response amplitude operator (RAO), using Abaqus. The RAO is a dimensionless response spectrum that, combined with the load spectrum, give the actual response. Using RAOs can only be done under the assumption that there is a linear relation between the load and the response. The RAO and the load spectrum can be used to create a frequency dependent stress response spectrum.

In the case of very large excitations, damping of the structure must be evaluated. Many types of damping exist. Mechanical and aerodynamic damping are the most

relevant, when considering the flare tower response. Mechanical damping represents the natural damping within the structure. Aerodynamic damping represents the relative air velocity change, with respect to the structure, as it oscillates. Appropriate damping values can be found from experimental testing of similar structures, often as fraction of critical damping. Implementation of damping can be done using Rayleigh damping. A mathematical convenient method, but with the downside that the damping varies with the load frequency.

The response spectrum created by combining the RAO and the load spectrum can be used to find the statistically expected stress maxima. This, in turn, is part of the capacity consideration of the structure.

The value of the mean wind can be found from hindcast data, for the relevant region. It is defined with respect to an averaging period of, i.e. 10 min at a height of 10 m. The 10^{-2} annual probability maximum wind speed can be found, resulting in loads corresponding to the ULS design criterion. Loads from the mean wind can be assumed static when the eigenfrequencies are high. This because fluctuations of the mean wind have high periods, and would not affect structures with high eigenfrequencies.

5.2 Wind pressure specter

The procedure for finding the frequency dependent 10^{-2} annual probability wind pressure $q_t(n)$ to be used in the Abaqus analysis is outlined below [6, 12.46].

$$q_t(n) = \frac{1}{2}\rho_{air} C_D \overline{U}^2 + \rho_{air} C_D \overline{U} \dot{u}(n) \tag{5.1}$$

The pressure is dependent on the height in addition to the frequency, but a reference height $z_e = 52m$ will be used as described in section 4. In equation 5.1 the first part represents the static wind load and the second part represents the turbulent wind load. It is calculation of the second part that is dependent on the load frequency, and will give dynamic response. In the equation, $\overline{U}$ is the middle wind speed, $\dot{u}$ the turbulent wind speed from the wind specter [7, 2.23] and C_D is the drag coefficient [8, 10.2.10].

$$\overline{U} = \overline{U}_R \left(\frac{z_e}{z_r} \right)^{\alpha} \tag{5.2}$$

Where the reference wind speed $\overline{U}_R = v_{b,0} = 43m/s$, as described in the National Annex of the Eurocode [5, 4.2, Figure NA.4(901.1)], $z_r = 10m$, is a reference height [6, p. 259] and $\alpha = 0,10$ is a surface roughness factor [6, Table 12.1].

$$C_D = C_D^s \left[1 - 0,015 \left(20 - \frac{h}{D(h)}\right)\right] \tag{5.3}$$

C_D^s can be found from "Wind effects on structures" [8, Figure 4.5.5.c] in combination with the Reynolds number. A diameter of D(h) = 3.65m is chosen, as calculated in section 4.4, for a height of h=43m above sea level.

$$\frac{1}{2}\dot{u}(n)^2 = S_{\dot{u}}(n)\Delta n \tag{5.4}$$

Where $S_{\dot{u}}(n)$ is the Kaimal wind speed specter [8, 2.3.21] and Δn is a constant difference between successive frequencies, given as 0,05 Hz.

$$S_{\dot{u}}(n) = \frac{200 \cdot f(n)}{(1 + 50 \cdot f(n))^{5/3}} \cdot \frac{u_\star^2}{n} \tag{5.5}$$

$$f(n) = \frac{n \cdot z_e}{\overline{U}(z_e)} \tag{5.6}$$

$$u_\star = \sqrt{k_{10}} \cdot \overline{U}_{10} \tag{5.7}$$

In these equations $f(n)$ is a non-dimensional frequency [8, 2.3.17], $u_\star$ is the wind shear velocity [6, 12.41b], k_{10}=0,0025, is a surface roughness parameter [6, Table 12.1] and $\overline{U}_{10}$ is the middle wind speed at 10m height.

The resulting wind pressure specter is shown in figure 5.1 as calculated by the Matlab script in appendix A.4. The 1,3 multiplication factor from table 3.1 has been included to be in accordance with the NORSOK standard.

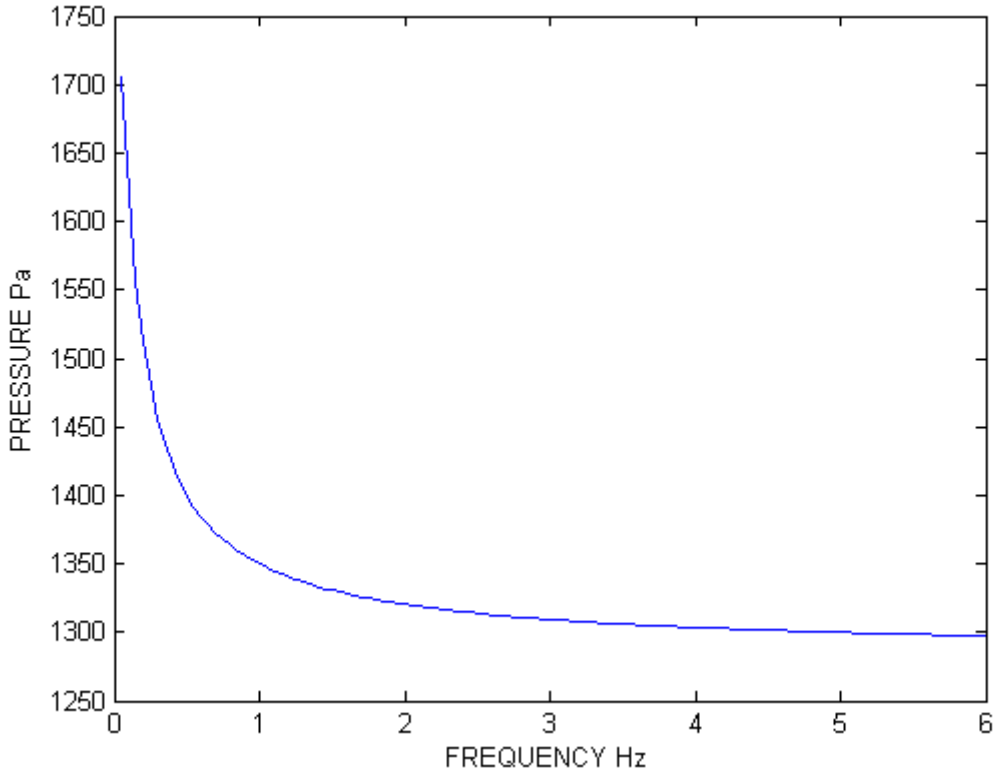

Figure 5.1: Wind pressure specter

As explained earlier, the wind load can be divided into two different parts, the static and the dynamic. Static wind pressure is 1282 Pa, as calculated using appendix A.4. That leaves the dynamic wind pressure specter, as showed in figure 5.2.

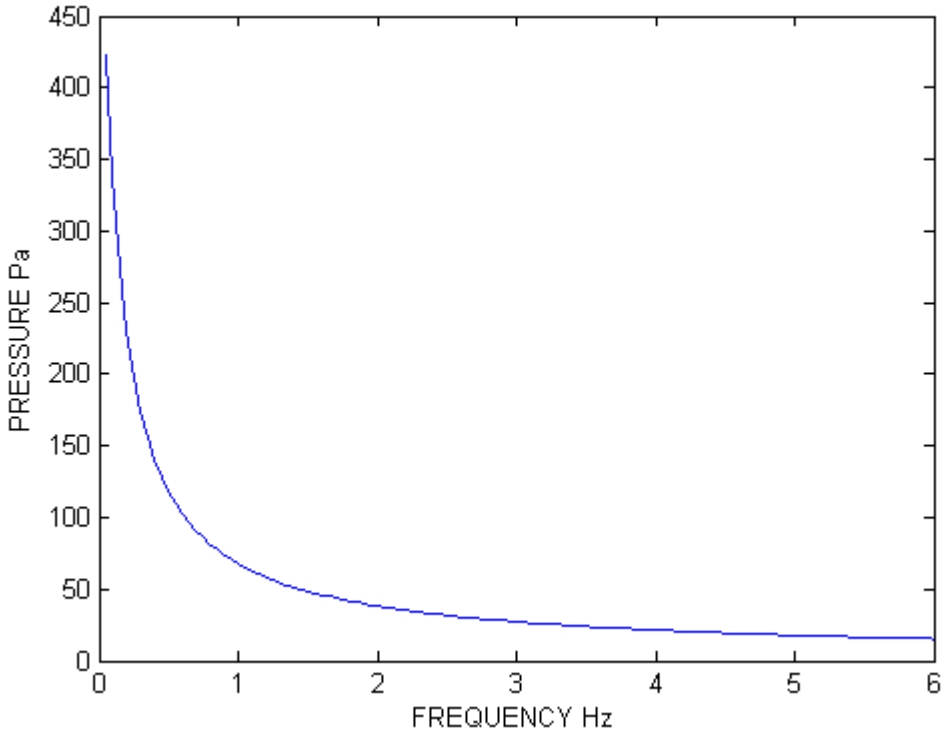

Figure 5.2: Dynamic wind pressure specter

5.3 Response amplitude operator - RAO

RAOs for different levels of damping have been calculated, as showed in figure 5.3. The calculations have been conducted in Matlab, as described in appendix A.5 According to a study of bottom supported offshore wind turbines [9, p. 8], the mechanical damping is 1% and aerodynamic damping is 4% of critical value. In this case the turbine blades will contribute a lot to the aerodynamic damping. This is not valid for the flare tower. The flare tower, on the other hand, will have an increased damping due to wind fluctuations in relation to the ventilation cut outs. It is assumed that structural damping of 1% and aerodynamic of 2% give realistic results.

Using Rayleigh damping, the critical damping fraction is divided into mass and stiffness damping, α_1 and α_2, respectively [6, p. 288].

$$\alpha_1 = \frac{2n_1n_2}{n_2^2 - n_1^2} \cdot (\lambda_1 n_2 - \lambda_2 n_1) \tag{5.8}$$

$$\alpha_2 = \frac{2(\lambda_2 n_2 - \lambda_1 n_1)}{n_2^2 - n_1^2} \tag{5.9}$$

Both λ_1 and λ_2 were considered equal to the same fraction of critical damping. The lowest structural eigenfrequency, n_1 = 1,44 and the highest, n_2 = 5,5 have been used. They where considered to give appropriate damping for all frequencies. This resulted in α_1 = 0,1141 and α_2 = 0,0144 for 5% of critical damping, and α_1 = 0,0685 and α_2 = 0,0086 for 3% of critical damping.

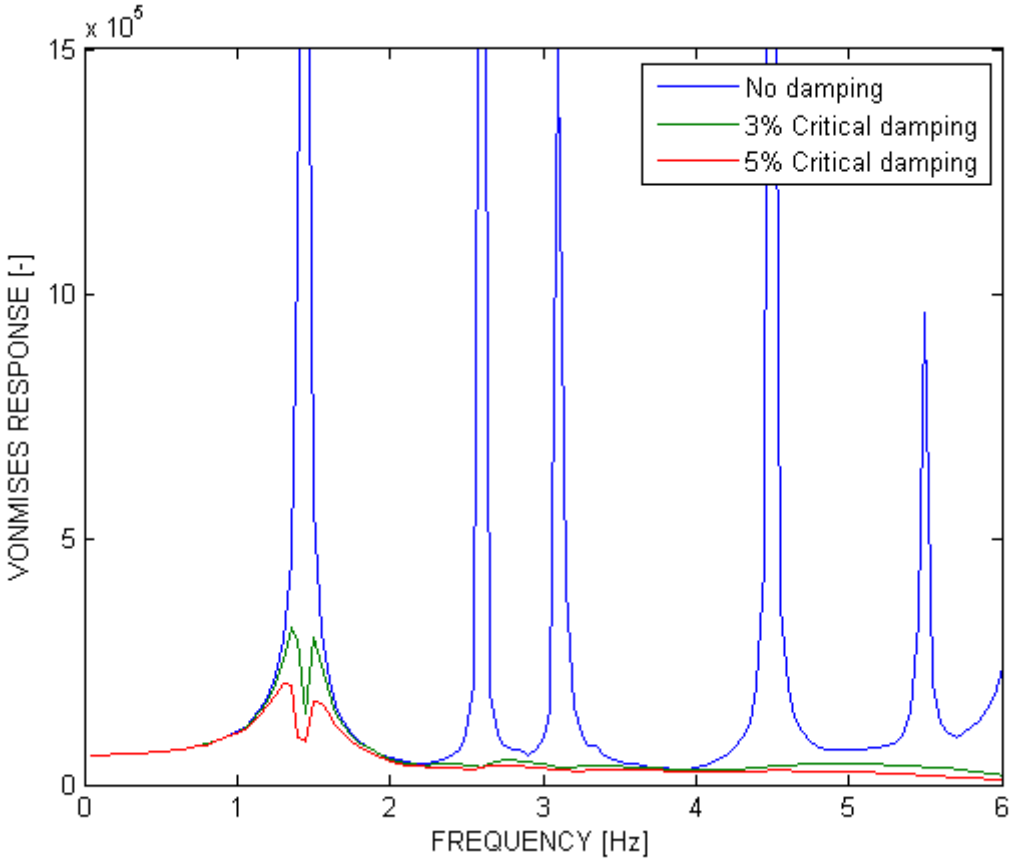

Figure 5.3: Dimensionless RAO specter

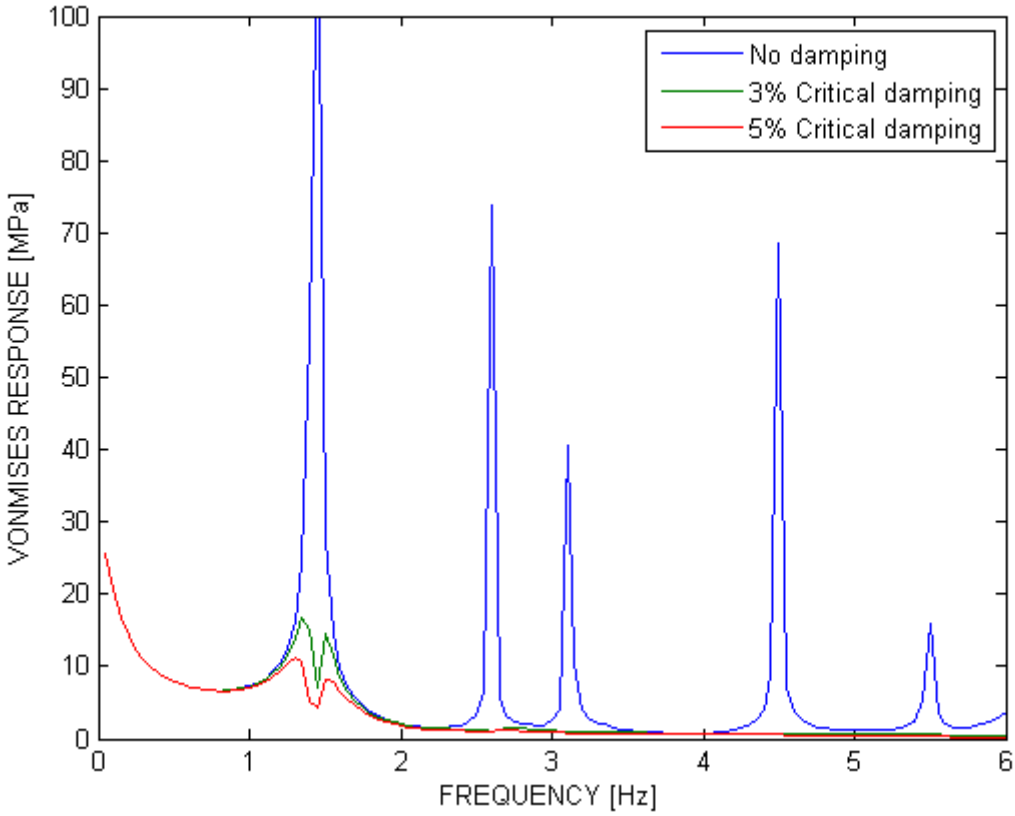

Figure 5.4: Stress response specter

In the two response specters shown in figure 5.3 and figure 5.4 the peaks are due to the different eigenfrequencies of the structure. The choice of 6 Hz as the upper limit where attempted, and proved reasonable. The reason for this is that the damped responses show that inclusion of higher frequencies would give negligible responses. At approximate frequency of 1,45 Hz there are two peaks in the damped specters, but only one in the undamped. The double peaks are due to there being two eigenfrequencies in close proximity, as shown in section 6.3. It is believed that the reason for there being only one peak in the un damped response, is that damping altered the resonance frequencies somewhat.

There is some danger that the mass damping part, of the Rayleigh damping method, causes an over-damping of the higher eigenfrequencies of the structure. The large response reduction of the high-frequency peaks could indicate this. No further investigation has been done, as these frequencies are located in the low energy part of the turbulence specter.

5.4 Statistic response values

Combining the wind pressure specter in figure 5.2 with the 3% of critical damping, RAO specter, from figure 5.3, give the actual response specter shown in figure 5.4. The combining of the two specters where done using the relation shown in equation 5.10 [7, 2.23].The specter has dimensions $[MPa^2]$.

$$S_{MPa^2}(n) = \frac{1}{2}(q_t(n) \cdot RAO(n))^2 \tag{5.10}$$

This specter can be used to find the largest expected stress in the structure, X_{max}, due to the dynamic wind load [13, 7.1.2]. The calculation of X_{max} was done using Matlab, as described at the end of appendix A.5

$$X_{max} = \sigma \cdot \left[\sqrt{2ln(n_\tau)} + \frac{0,57722}{\sqrt{2ln(n_\tau)}} \right] \tag{5.11}$$

Where σ is the standard deviation of the specter and n_τ is the expected number of global maxima during a load period of $\tau = 10$ min.

$$n_\tau = \frac{60 * \tau}{t_0} \tag{5.12}$$

Where t_0 is the zero up-crossing period of the specter. σ and t_0 can both be found using the spectral moments m_0 and m_2.

$$\sigma = \sqrt{m_0} \tag{5.13}$$

$$t_0 = \sqrt{\frac{m_0}{m_2}} \tag{5.14}$$

The spectral moments are found integrating the response specter as shown in equation 5.15.

$$m_i = \int_0^\infty n^i \cdot S_{MPa^2}(n) dn \tag{5.15}$$

Chapter 6

Modeling using Patran Pre

Even though the analysis will be conducted using Abaqus, the modeling itself has been done using Patran Pre. The reason for this is that Patran Pre is superior to the Abaqus preprocessor when it comes to modeling shell elements. It is also great with regards to mesh control. Both Martin Storheim, PhD at Marin and Frank Klæbo at Sintef Marintek have been of great assistance regarding the use of Patran.

All modeling in Patran has been saved as Sessions and posted in the appendices, either as .ses files or the Matlab files used to make the .ses files.

6.1 Structural design

This will be a brief description of how the structural parts of the flare tower have been modeled in Patran.

6.1.1 Shell and ventilation

The surface of the flare tower was divided into a large number of smaller shell plates when designed in Patran.

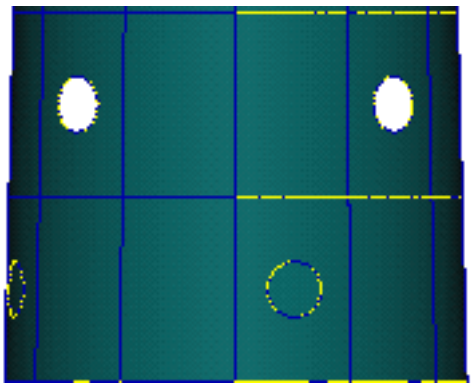

Figure 6.1: Shell and ventilation modeling

The reason for this is to make it easier for the program to divide and number the resulting surfaces as they are made, after the creation of the cut outs. Making cut outs with the entire surface in one piece proved both difficult and highly time consuming.

As a result of the need to create a large number of surfaces, the modeling became highly repetitive. Instead of creating every surface section one at a time, the Matlab script A.1 was made. It uses command lines originally written by Patran, and copies them into many similar ones, but with different numbering of points, distances, curves and surfaces. It start with points, that are linked by curves and finally creates surfaces between the curves.

The ventilation cut outs are made in a similar way, using Matlab script A.2. A large number of circular holes are to be cut from the surfaces in a specific pattern. In this case, getting the numbering correct is very important, as the shape creating the cut out must be linked to the correct surface.

6.1.2 Material properties, boundary conditions, additional equipment and damping

How the material properties, boundary conditions and addition equipment have been implemented in Patran is shown in appendix B.1.

The material properties are as described in section 2.3. Young´s modulus, density and Poisson´s ratio have been implemented in Patran, while the yield strength will be used as capacity when comparing the stresses from the analysis and for plasticity analysis. The material type was defined as linearly elastic homogeneous steel up to the yield strength where it was defined as perfectly plastic.

Young´s modulus	2.05 x 10^5 N/mm^2
Density	7850 kg/m^3
Poisson´s ratio	0.3
Yield strength	309 MPa

Table 6.1: Material properties

The boundary conditions were defined as nodal displacements with predefined displacements of 0 translation in x,y and z-direction, and 0 rotation about the x,y and z-axis. The reason for the choice of boundary conditions are described in section 2.5

In addition to the shell there are some equipment connected to the tower. This is the flare pack, piping and ladder as described in chapter 2.1. These have been modeled as 0-dimensional masses. The mass from the flare pack was divided into 12 submasses of 208 kg, distributed along the top edge of the tower. It is divided in such a way since the method of connection, in reality is unknown. The masses from the piping and ladder have been divided into 26 submasses of 308 kg each. They were distributed along the edge of the tower, from top to bottom, where this equipment is assumed to be fastened.

The point masses that were applied to the structure had to be linked to the analysis using point elements. This was in addition to the regular meshing of the structure.

Damping of the structure was included using Rayleigh damping, as described in section 5.3. The damping applied for the final analysis were 3% of critical damping, divided into factors α_1 and α_2 with values 0,0685 and 0.0086, respectively. Damping were included in Patran, using the material properties section, as mass proportional and stiffness proportional damping.

6.1.3 Meshing

The initial mesh were made by using triangular three node elements and a hybrid mesher with approximate element size of 0,2 m. The Patran input for the meshing are shown in appendix B.2.

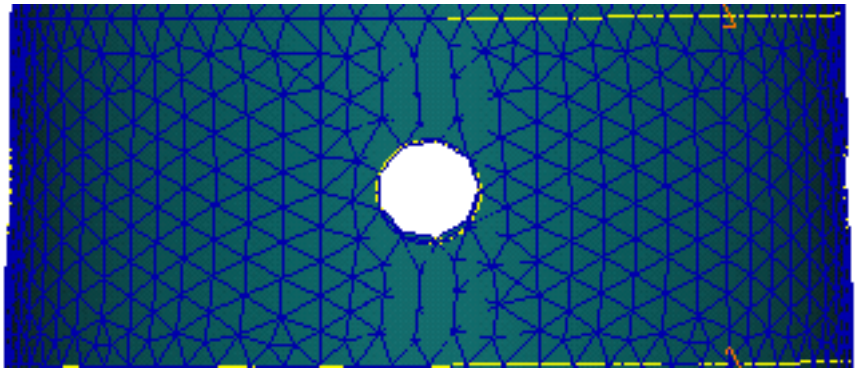

Figure 6.2: Initial element size

The choice of element size is connected to the size of the smallest relevant structural detail in the structure. In this case that is the ventilation cut outs. With a cut out diameter of 0,6m the elements would have to be small enough to replicate a somewhat circular shape without there being disfigured elements. With the choice of approximate elements size of 0,2m the element mesh became as in figure 6.2. This shows that the choice of mesh size was sufficient, at least for the initial calculations. This element size give number of nodes and elements as shown in table 6.2.

Nodes	16025
Elementes	31211

Table 6.2: Nodes and elements

6.2 Loads

This will be a brief description of how the loads on the flare tower have been modeled in Patran.

6.2.1 Inertia loads

The masses in the structure are affected by gravity and platform accelerations, as described in section 3. In table 3.6 the gravitation and platform accelerations are multiplied with action factors. This is done to be in accordance with the standards [1]. When applying the accelerations to the model, the 15° angle must be taken

into consideration. This is because the structure has been design as if vertically straight, for easier modeling.

X-dir $= 9.81 \cdot sin(15) = 2,54 m/s^2$
Z-dir $= 9.81 \cdot cos(15) = 9,46 m/s^2$

Table 6.3: Permanent acceleration

X-dir $= 1,66 \cdot cos(15) + 2,34 \cdot sin(15) = 2,21 m/s^2$
Z-dir $= 2,34 \cdot cos(15) + 1,66 \cdot sin(15) = 2,69 m/s^2$

Table 6.4: Platform movement

The combination of upwards platform movement and downwards gravity is chosen, as this is the worst case scenario. For the calculations to be strictly correct, the platform movement should be modeled as dynamic. From appendix C.1 and C.2 the platform movement periods are shown to be in the vicinity of 6 - 20 seconds. This is far away from the eigenfrequencies of the flare tower, and dynamics related to them have been considered irrelevant.

Directions	X	Y	Z
Accelerations	4,75	0	12,15

Table 6.5: Acceleration field

The acceleration field from table 6.5 has been modeled in Patran as two different static inertia loads, one targeting the mass of the structure and the other targeting the additional masses from the flare pack, piping and ladder. The input for Patran is shown in appendix B.3.

6.2.2 The Eurocode wind load

The Eurocode approximation of the wind load, as described in section 4, is independent of the load frequencies. By use of the construction factors $C_s C_d$ and the force factor c_f an approximation of the dynamics from wind turbulence, structural response, damping and wind flows was made. As a result the wind pressure from this method can be used in a static analysis, instead of dynamic, giving a quick and easy calculation in Abaqus. The load has been modeled as a static pressure load working on one side of the tower. The pressure of 2688 Pa, as calculated from table 3.6, was included in Patran by applying a uniform pressure on one half of

the structure, on the opposite side of where the inertia loads where located. The input is shown in appendix B.3.

6.2.3 Wind specter load

In the case of the Kaimal wind energy specter approach a frequency response specter was made using Abaqus. As input for the Abaqus analysis a homogenous unit pressure load of 1 [-] was applied in Patran as showed in appendix B.4. Harmonic frequencies were chosen in the range of 0,05 - 6 Hz with frequency steps of 0,05 Hz. In one case some adjustments were made to give a more correct response curve. Three curves were made using 5% and 3% of critical damping, and no damping. The one with 3% damping were used in the capacity analysis, as described in section 5.3. The largest stress response for each frequency were taken from the Abaqus results and plotted using Matlab. The plotted curve where then used in the results analysis.

6.3 Eigenfrequency analysis

As previously discussed in section 5.3, the eigenfrequencies are important when considering the structural response due to dynamic loading. Knowing these frequencies are helpful when comparing dynamic analysis results from Abaqus, with the expected locations of response peaks. They where also used when calculating the quasi-static analysis related to the Eurocode approximation. They will further be used when considering the effects of possible VIV, in section 8.

Mode no.	1	2	3	4	5	6	7	8	9	10
Eigenfreq.	1.435	1.445	2.596	2.859	3.123	3.339	4.494	5.170	5.487	6.054

Table 6.6: Eigenfrequencies

In Patran there is an analysis mode for the calculation of eigenfrequencies. No loads need to be included, just the structure and the boundary conditions. The desired number of eigenfrequencies to be calculated are given as input for the Abaqus analysis. 10 eigenfrequencies where calculated, as shown in table 6.6. This number where considered sufficient to cover the largest dynamic responses, which proved to be correct, as described in section 5.3.

Chapter 7

Abaqus results

7.1 General

A matrix showing the different types of analysis that are to be conducted is displayed in table 7.1.

	Quasistatic	**Dynamic**
Linear	Eurocode approximation	Wind specter
	Mesh refinement	
Non Linear	Buckling	
	Plastic analysis	

Table 7.1: Case matrix

A quasi-static analysis will be conducted, using the wind pressure acquired from the Eurocode procedure in section 4. A dynamic analysis will be conducted using the wind specter procedure from section 5.

Static loading will be used to examine different types of effects. Applying wind load, giving stresses that surpass the 309 MPa material limit, to examine how plasticity would spread in the material. The largest stresses from either the quasi-static or the dynamic load case will be used to check the effect of mesh refinement and buckling. All these three analysis will be run as static, with the stress corresponding wind pressure applied.

7.2 Eurocode approximation

The quasistatic analysis has been run with the inertia loads and the Eurocode wind pressure as loading. The inertia loads are a result of the accelerations described in table 3.6, summed up in an acceleration field given in table 7.2. A wind pressure of 2688 Pa is used, also from table 3.6.

X	1,66 m/s^2
Y	0 m/s^2
Z	12,15 m/s^2

Table 7.2: Inertia load acceleration field

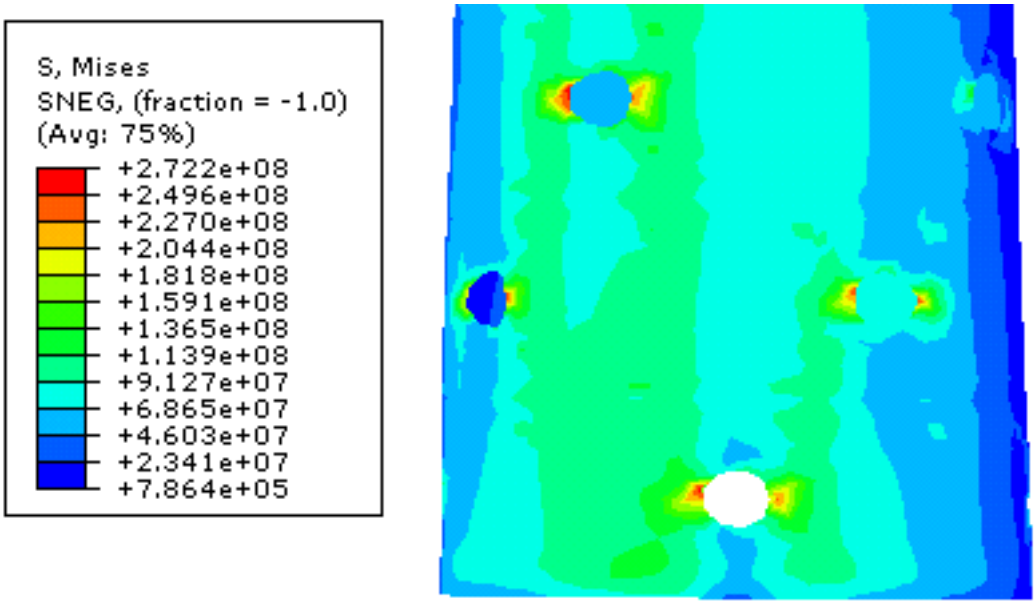

Figure 7.1: von Mises stresses

Figure 7.1 show the flare tower from the compression side, where the largest stresses are found. It shows that the critical stress areas are located at the horizontal edges of the ventilation cut outs. The maximal stress level in the structure is 2,722e+08 = 272 MPa<309 MPa, that is the accepted yield strength of the chosen steel, as described in section 2.3. It is also shown that the maximal stress level can be found in multiple areas in the structure, not just one.

7.3 Wind specter analysis

The wind specter analysis consists of three parts: Inertia loads, static wind pressure and dynamic wind pressure. They have all been analyzed separately, giving the sum of these as the final result. This is done as it is assumed that the response is linearly related to the loads.

The inertia load accelerations used for the analysis are described in table 7.2. The largest stresses occur, as previously shown in section 7.2, in the corners of the ventilation cut out. Inertia load results are shown in figure 7.2.

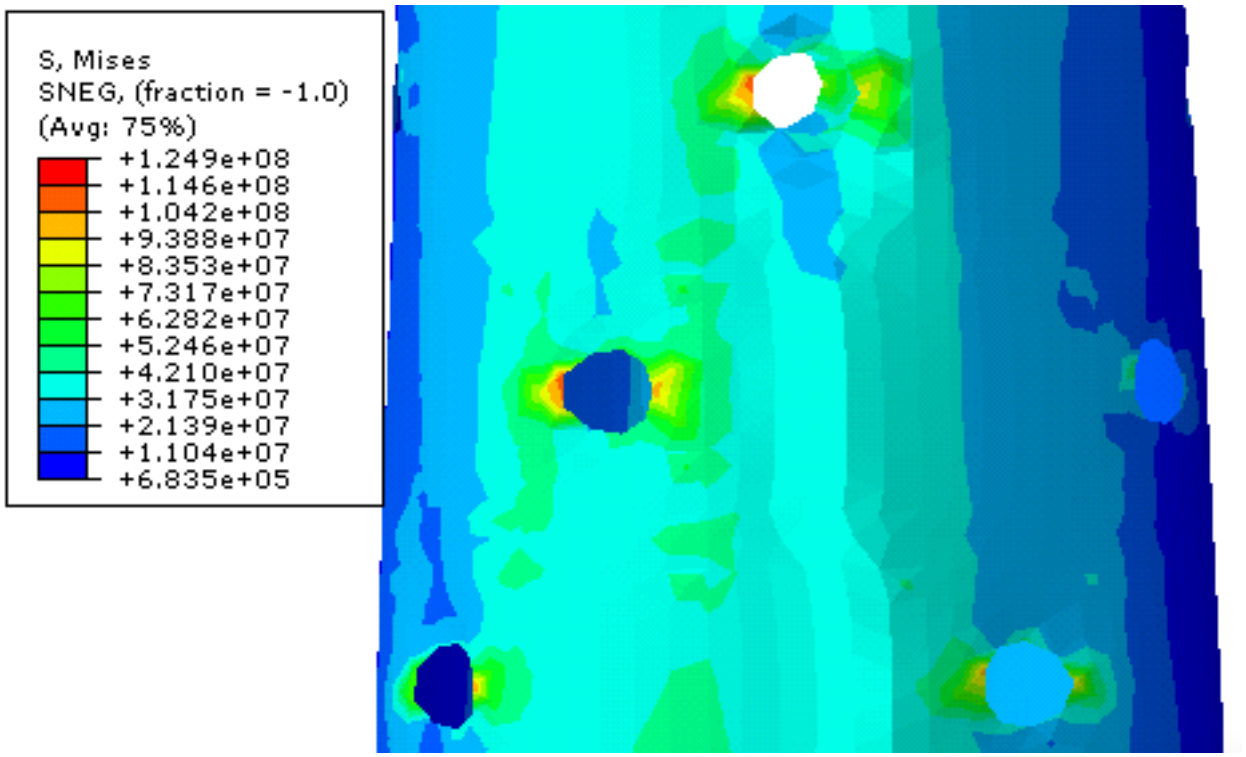

Figure 7.2: Stress from Inertia loads

The static wind load of 1282 Pa is used for the analysis, as described in section 5.2. This is the part of the wind with fluctuation frequencies well below the eigenfrequencies of the structure. Static wind load results are shown in figure 7.3.

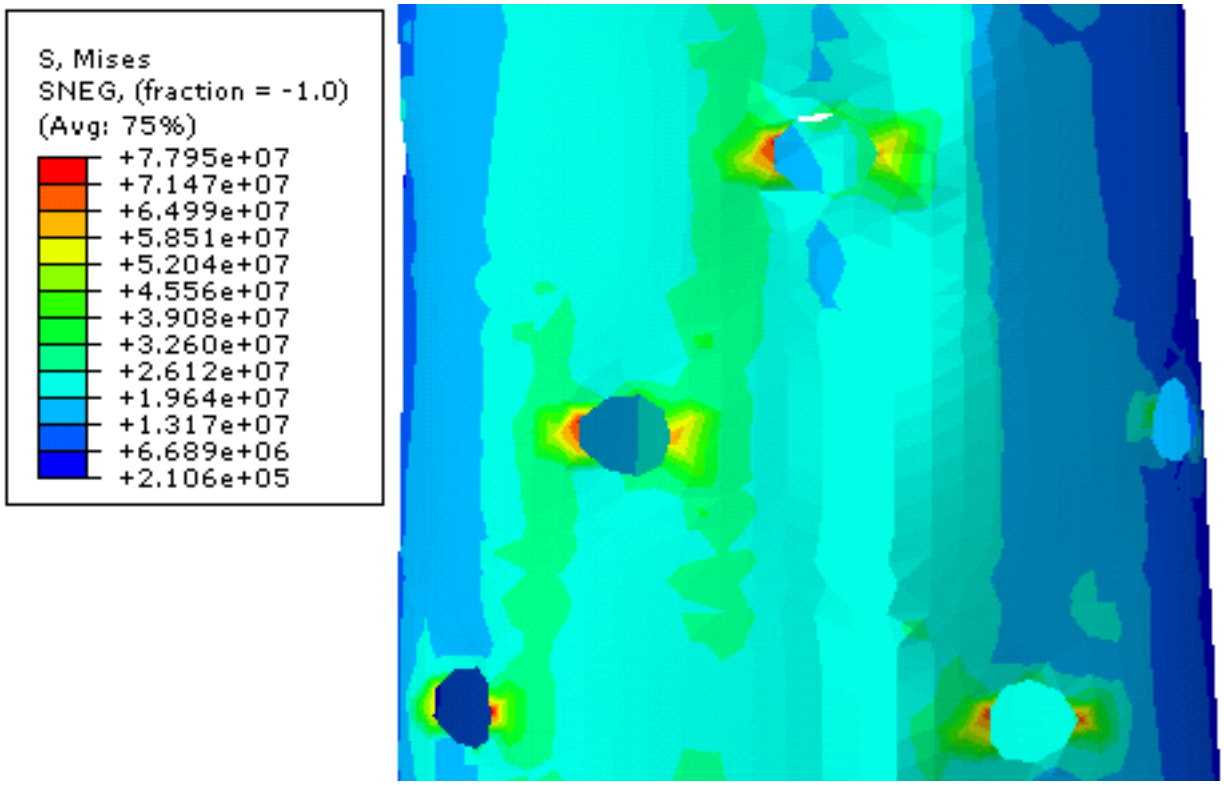

Figure 7.3: Stress from static wind load

Stress from the dynamic wind load is found using the description in section 5.4. The statistic largest stress response have been found analysing the response specter shown in figure 5.4. The Matlab script found in appendix A.5 give $X_{max} = 38$ MPa.

Inertia load	125 MPa
Static wind load	78 MPa
Dynamic wind load	38 MPa
Sum	241 MPa

Table 7.3: Wind specter loads

Wind specter analysis loads of 241 MPa<309 MPa, that is the accepted yield strength, as described in section 2.3.

7.4 Plastic analysis

A plastic analysis where run to examine how plasticity would spread in the structure. It has been identified that the ventilation cut outs on the compression side are the most vulnerable, which was the case for plasticity as well.

A wind pressure of 6000 Pa was applied to the structure, instead of the 2688 Pa from the quasi-static analysis. This was done to be certain there would be plasticity in the structure. A maximum of ten load increments, using an initial increment step of 0,1 where used. Prior to each new load increment Abaqus evaluates the results from the previous increment and decides the size of the next. Each increment applies a fraction of the total load, approaching a load value of 1.0.

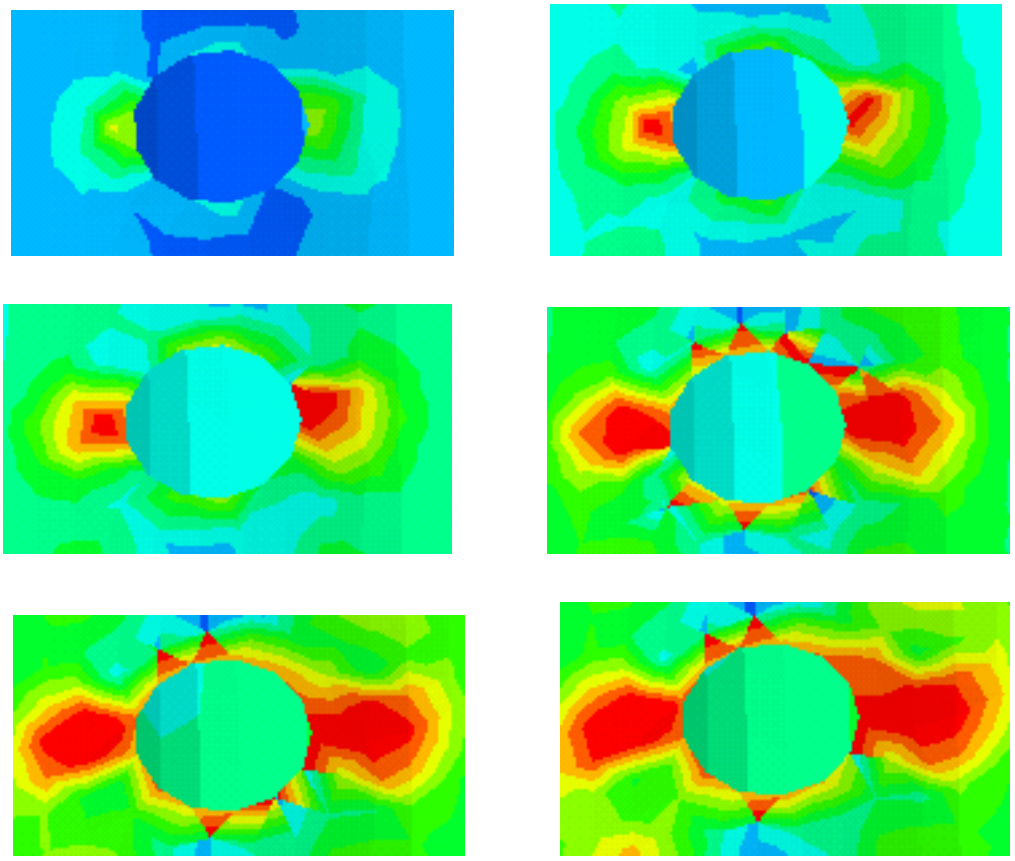

Figure 7.4: Plasticity in the ventilation cut out area

Figure 7.4 show how the plasticity spreads in relation to a ventilation cut out. As is shown, the plasticity spreads horizontally away from the cut out, into the rest of the structure. A lot of the energy is also distributed along the edge of the cut

out, and vertically from the horizontal spread.

7.5 Mesh refinement

To check wether the size of the elements used in the analysis are sufficiently small, mesh refinement were performed. The initial element size where given as 0,2m, a size that appeared to give sufficiently small elements to replicate the model. In the mesh refinement there are a sequential doubling of the number of elements in the model, starting from half the number initially chosen, and resulting in 16 times that number.

Element size [m]	# Nodes	# Elements
0,3	7987	15298
0,2	16025	31211
0,14	30905	60494
0,1	60354	118616
0,07	124189	245320
0,05	237411	470476

Table 7.4: # Nodes and elements according to element size

Examples of the element size compared to the ventilation cut outs are shown in figures 7.5 and 7.6, for the largest and the smallest elements respectively. The ventilation cut outs are 0,6m in diameter.

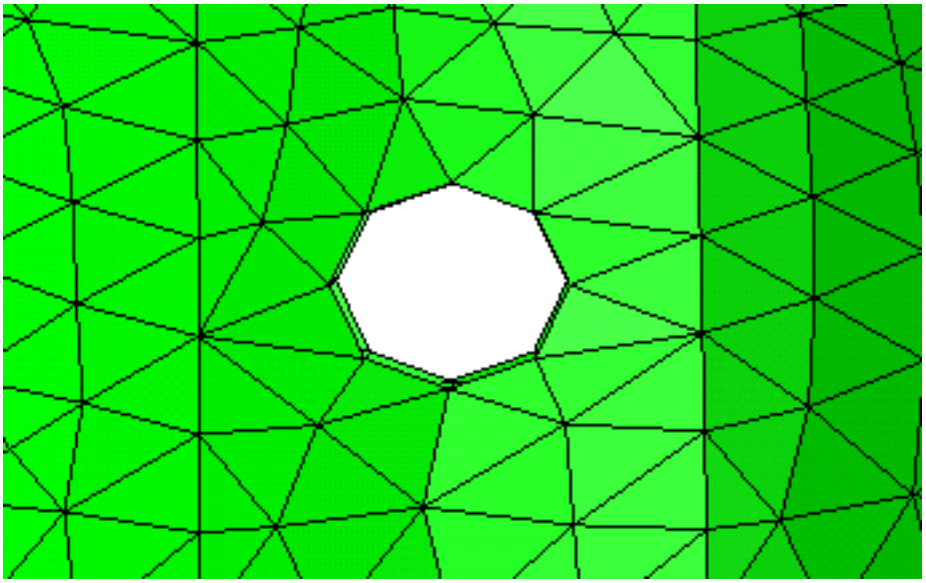

Figure 7.5: Element size 0,3m

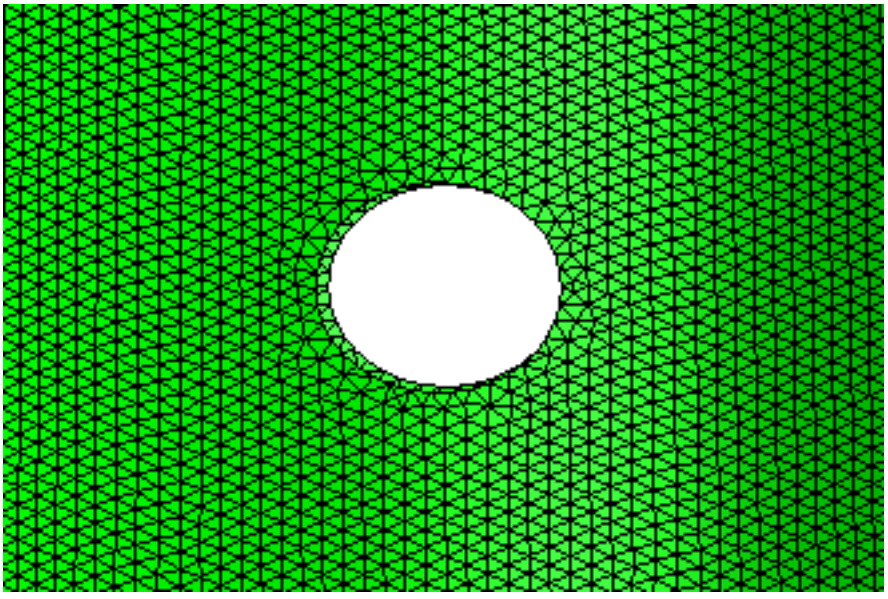

Figure 7.6: Element size 0,05m

Stress for the refined meshes are shown in figure 7.7.

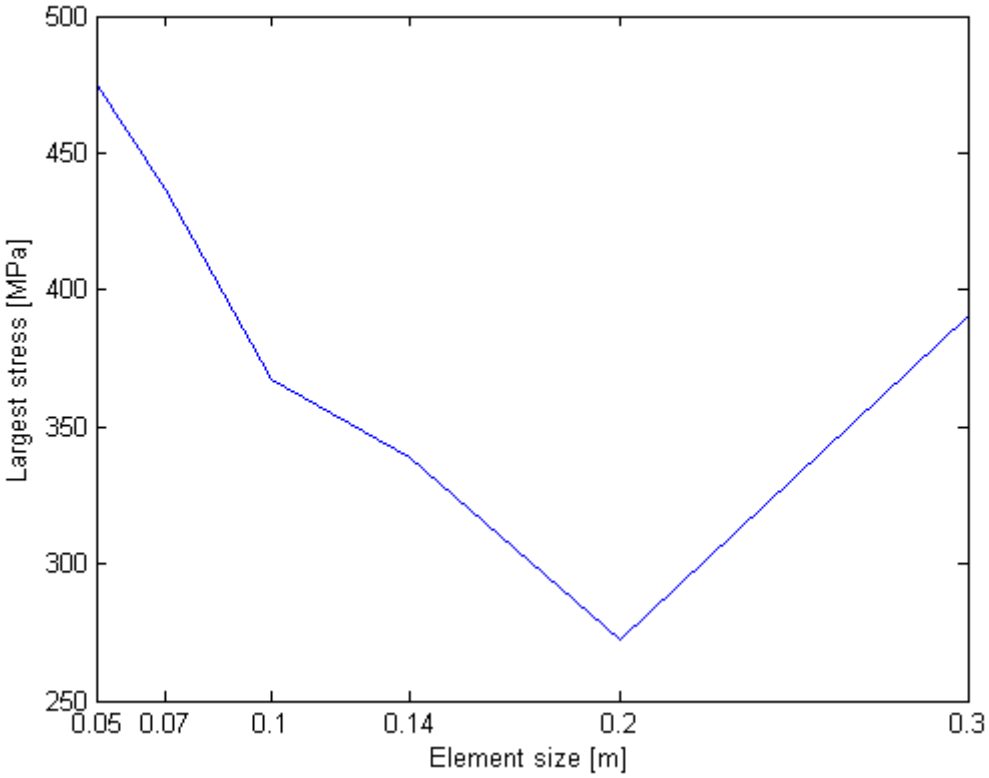

Figure 7.7: Stress according to mesh size

Figure 7.7 show the largest stresses in the structure for the corresponding shell size. There is an increase on stress both for lower and higher number of elements, than the size originally used.

7.6 Buckling analysis

Compressions in the structure might cause different kinds of buckling. As shown in the items of figure 7.8, the structure seem to be sensitive to local shell buckling in the ventilation cut out areas. Local buckling might not be as big a problem as global buckling, but the effect must be evaluated. Design changes that might be considered are thicker shell, stiffening in longitudinal and/or circumferential direction or removal of the most exposed ventilation cut outs.

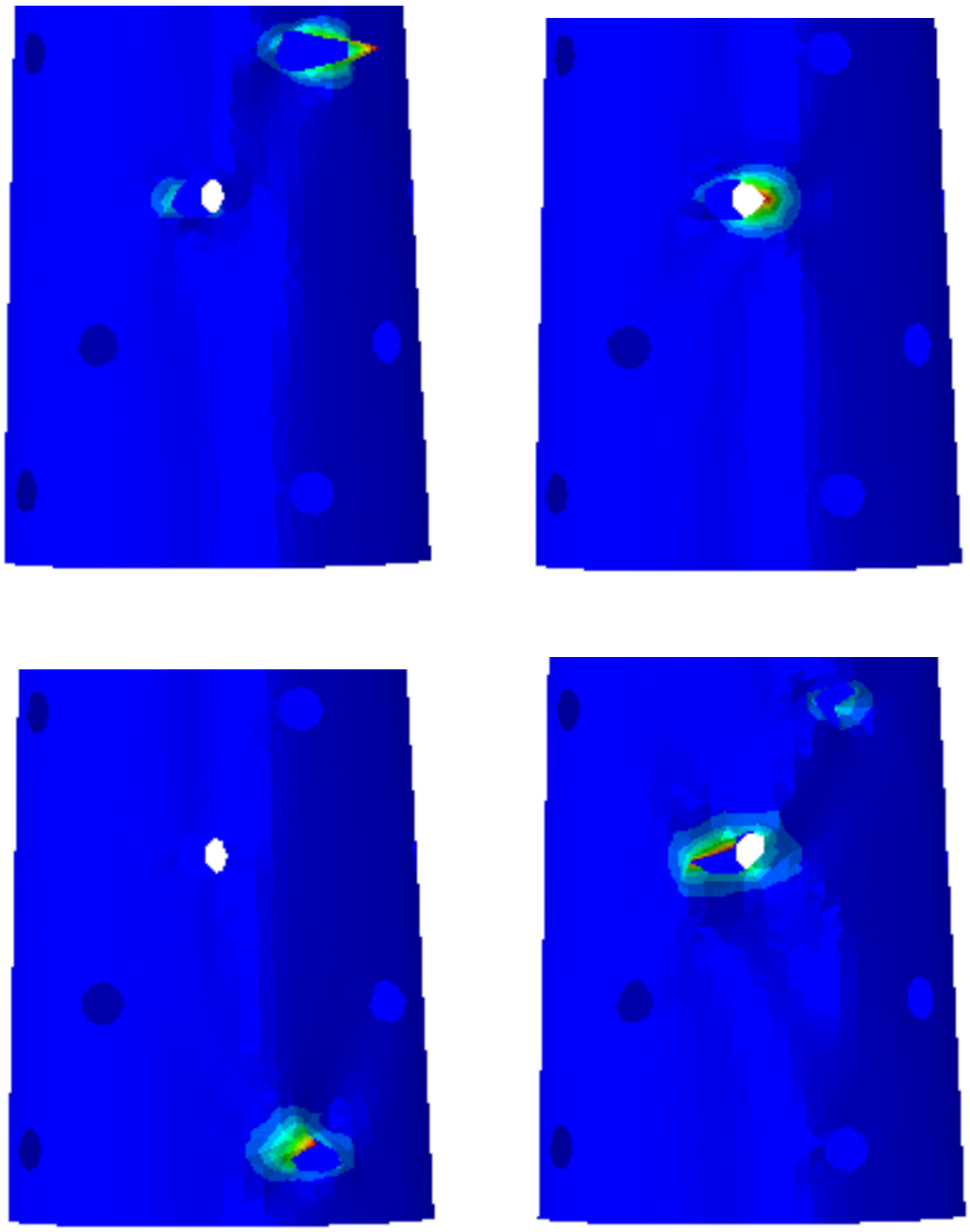

Figure 7.8: Local shell buckling

Chapter 8

Vortex Induced Vibrations

8.1 General

One aspect related to wind dynamics is vortex induced vibrations (VIV). This is a phenomenon created by pressure change due to vortices created in the wake of the structure. VIV causes vibrations in the structure that can be problematic both in respect to strength and fatigue. It is troublesome, especially for circular structures. The principles of VIV are outlined in this section.

8.2 Principles of VIV

The tower is subjected to loads from the air flow. These forces can be divided into viscous, pressure lift and drag forces consisting of skin friction (viscous drag) and form drag (pressure drag) [11, p.7]. Together they give in-line and cross-flow force components on the structure.

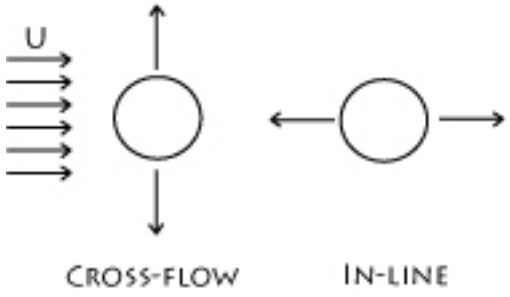

Figure 8.1: Cross-Flow and In-Line vibrations

As the air flow increases in speed, vortices are shed from the surface of the cylinder, in the air flow wake. When the Reynolds number reaches 40 the vortices start shedding from alternating sides.

Figure 8.2: Vortex shedding

These changes in air flow cause the pressure resultant for the tower to change as the vortices are shed. As described in Bernoulli´s equation [7, 2.4], the pressure in a medium is inversely related to the speed of the medium. When the speed increases the pressure goes down, and vice versa. This means that as the flow halts to create a vortex the speed decreases and the pressure increases. This change effects the pressure in both in-line and cross-flow direction. As the vortex is released and another is created on the opposite side, the pressure alternates. The resulting forces from the pressure changes give vibrations in the structure for the in-line and cross-flow directions. The frequency that the tower will vibrate in will be related to the vortex shedding frequency, f_v.

$$f_v = \frac{U}{D} * St \tag{8.1}$$

Where U is the wind speed, D is the tower diameter and St is the Strouhal number, a function of the Reynolds number. This results in dynamic loading even if there is steady state air flow.

As for all structures subjected to dynamic loading, the tower is sensitive to frequencies close to the eigenfrequency. If the vortex shedding frequency approach the eigenfrequency it might cause large responses, even if the wind energy is low. An additional problem is related to the "lock-in" phenomenon. When f_v approaches the eigenfrequency f_n, f_v "locks on" to f_n, as described in figure 8.3. As a result the vortex induced vibrations will be in resonance with the structure even as the wind speed increases. This will largely increase the number of wind speeds that will cause large dynamic loads in the structure.

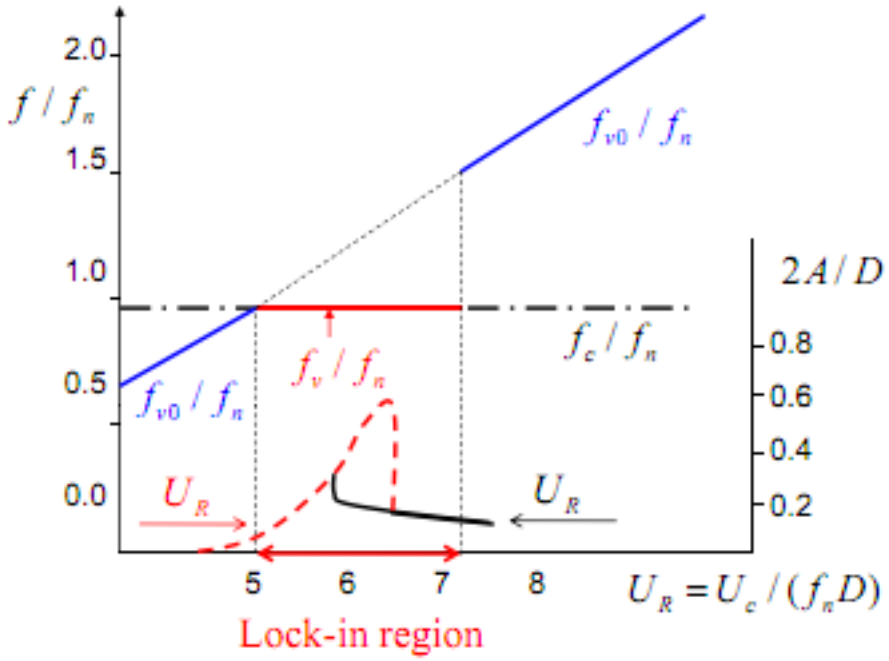

Figure 8.3: Lock-In

"Lock-in" will occur for reduced velocities of $5 < U_R < 7$, where U_R is defined as:

$$U_R = \frac{U}{f_n * D} \tag{8.2}$$

8.3 VIV calculations

Since the Reynolds value of 40 is very low, the flare tower would be affected by VIV. The more interesting question is wether the VIV frequencies are close to the main eigenfrequency of the structure, and could cause the occurrence of "lock-in". It is not necessarily the highest wind speeds that would cause VIV "lock-in". As argued earlier, resonance can cause large dynamic responses even for low energy wind loads. Using wind speeds varying between 20 and 40 m/s, and $f_n = 1,44$ Hz, given in table 6.6, U_R can be calculated as a function of the tower height. The structure diameter changes from 5 m to 2.3 m along the height of the tower, with a rate of change of 0,05 meters/meter. From this the reduced velocities can be found.

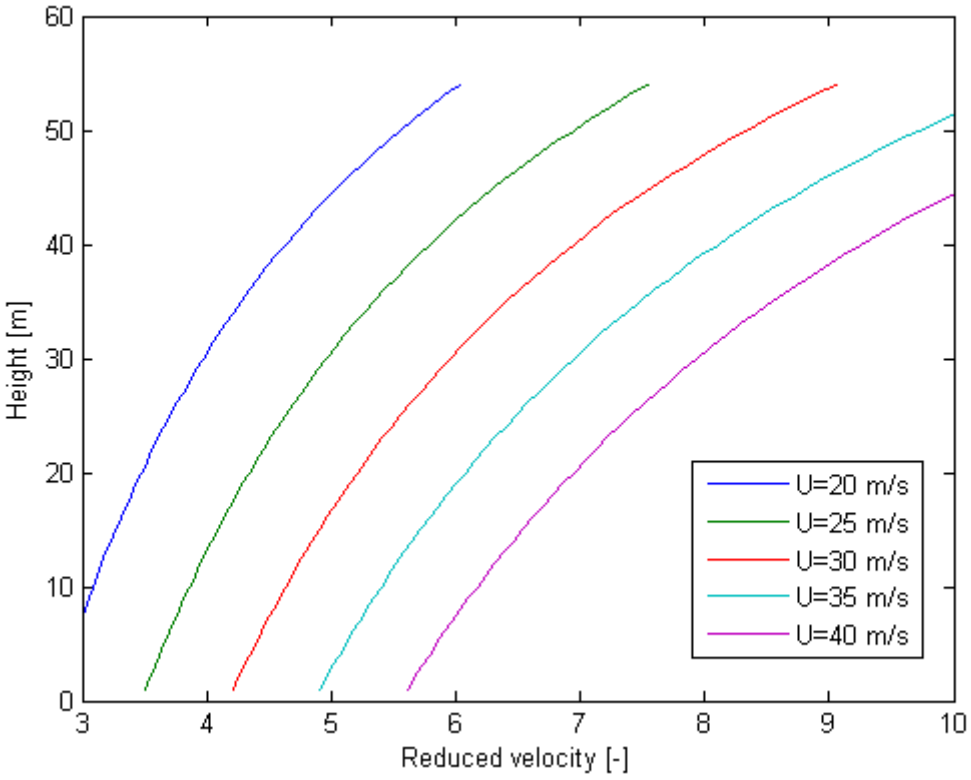

Figure 8.4: Reduced velocities for varying wind speeds

As shown in figure 8.4, all of the examined wind speeds would cause "lock-in" in some part of the tower. Wind speeds between 20 and 30 m/s are especially dangerous, as they would give resonance in large parts of the upper structure, and still contain a lot of wind energy. These results show that VIV is a major concern for the flare tower.

8.4 Counteracting VIV

There are mainly two ways of counteracting the effects of VIV. Damping and disrupting the vortex generation. As previously discussed in section 5.3, damping of the structure has been assumed to be 3 % of critical damping. This gave a substantial response reduction, as shown in figure 5.4. This damping would also reduce the dynamic response caused by VIV. Ways of increasing the damping of the structure could be considered.

The other measure that can be used is attempting to disrupt the vortex generation. One way for this to happen is to have other types of dynamic response in the structure. If a dynamic wind load forces the tower to vibrate in a different frequency than the one created by the vortices, it would serve as a disruptor of the vortex shedding. The second way of disrupting the vortices are to alter the surface of the structure, either by adding or removing parts. This is one of the purposes of the helical ventilation cut outs. The assumption is that the cut outs would give a VIV reducing effect, similar to that of helical strakes used on metal factory chimneys. This by allowing wind to flow through and disrupt the formation of vortices.

It has been difficult to find literature supporting the effect of the helix in suppressing VIV. A study looking at the effect of water jets in different patterns [11] states that: *"Configuration with jets in a helical pattern proves to give a very good VIV suppression performance"*. Whether or not this is relevant for the flare tower is unknown. An analysis of this would have to be conducted in a proper model test or simulation software.

Chapter 9

Discussion and further work

9.1 General

This section will include discussions concerning the different results presented in section 7. It will also present a list of further work to be conducted in case of a follow up of the novel flare tower design.

9.2 Quasi-static and dynamic analysis

Results from both quasi-static and dynamic analysis show that the structure has sufficient strength for the ULS consideration. The margin is not substantial, so a decrease of shell thickness would not be recommended, at least not in the lower parts of the tower. The upper parts could probably be decreased somewhat, since there are few high-stress areas here.

To be allowed to use the design, an accidental limit state (ALS) consideration must be performed. This requires a load with 10^{-4} annual probability wind pressure, without the structure sustaining substantial failure. None of the load factors described in table 3.1 should be included in an ALS consideration.

9.3 Mesh refinement

Figure 7.7 show some surprising results. Refinement of mesh will normally converge towards a correct value. In this case it seems to increase far beyond the initial

maximal value. In addition, the value increases with a decrease of elements. Both of these results are unexpected.

When calculating the stresses in relation to a circular cutout the largest expected theoretical value is $\sigma_{max} = 3\sigma_0$ [14, 10.2]. When checking wether this relation is applicable in this case a check has been done to find the stress at the edge of the cut out and at a distance above, not affected by the cut out.

Element size	Cut out stress	General stress	Multiplication factor
0,3	367	83	4,42
0,2	262	83	3,15
0,14	322	83	3,88
0,1	341	83	4,11
0,07	428	83	5,16
0,05	422	83	5,08

Table 9.1: Stress multiplication factor

This show that the multiplication of the general stress is much bigger than the theoretical maximum. Every elements size, except the initial, give to large multiplication. There can be several reasons for this.

If the cut out is elliptic the multiplication factor is multiplied with $\frac{1}{2}(1+\frac{a}{c})$, where 2a is the largest and 2c is the smallest diameter of the ellipse. This would cause the multiplication to become larger than 3. Deformation of the structure could cause the cut out to assume elliptic shape.

Another possible explanation is stress concentration. As the structure deforms the cut out will not remain perfectly circular, and could bend out of plane. Locations where the stresses could concentrate would appear, in comparison to a circular shape where the stresses are evenly distributed. This in turn would create "hot spots" in the structure, giving indefinite stress values for a FE analysis. Such a situation could explain why the stresses increase as the elements become smaller. Increasing the accuracy of the calculation of a singular point would give ever increasing stress. In reality, the hot spots would give increased stress, but far from the ones seen in the analysis. In a real structure, "hot spot" stress would be distributed more evenly over the cut out surface.

Stress concentration could also be the reason why the stress increased even when the element became larger. When displaying the element stress, Abaqus chooses by default to use nodal values. One can instead choose to use the middle of the element, by applying centroid evaluation.

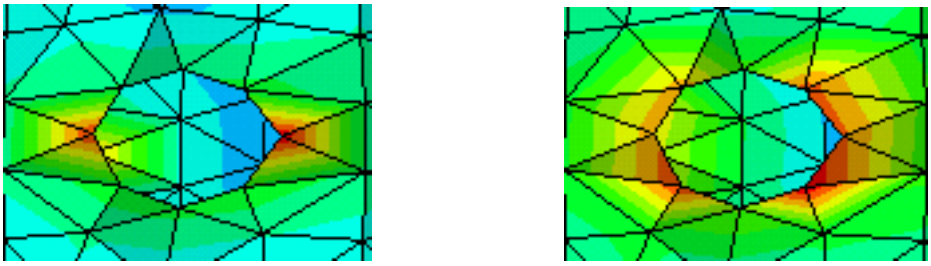

Figure 9.1: Nodal and centroid stress value

The left item in figure 9.1 show that the element nodes are located exactly where the stress concentration would occur. As a result, the stress that should be distributed along the edge of the cut out is concentrated in a singular spot. When applying the centroid method, as shown in the item to the right, the stress is more evenly distributed along the edge, as would be expected. The highest stress in the structure using the centroid method is 295 MPa, for the 0,3 meter element size.

Based on a theoretical maximum of $3 \cdot 83$ MPa $= 249$ MPa, it would not be too un-conservative to say that the initial stress value of 272 MPa is likely. There will still be the possibility of stress concentrations, but they are probably not as large as previously shown. The largest danger would be related to fatigue in these areas.

9.4 Plastic analysis

As discussed in the mesh refinement section, stress concentration might be the cause for high stresses appearing when the mesh is refined. Even though these values might be larger than in reality, stress concentrations would be a problem, as the structure deforms. In case of plasticity due to these stresses, the plasticity development is important to know. As shown from the results in figure 7.4, stresses would not remain concentrated, but would spread in structure. This is positive, since spreading the energy more evenly, reduces its potential for further strength reduction of the structure.

As the material chosen for the plastic analysis is defines as perfectly plastic, there would be no material hardening. In reality steel hardens as it is deformed plasticly, increasing the strength of the structure.

9.5 Buckling

As described in section 7.6, there are difficulties with local shell buckling related to the ventilation cut outs. The kind of buckling predicted would not in itself cause failure of the structure. The consequence would be large cracks in the shell, decreasing the structural strength and render it in danger of rapid fatigue failure. This because fatigue life is closely linked to the size of initial cracks.

Buckling occur in these areas because the shell is deformed by the global compression, as shown in figure 9.2. The cut out surface bends out-of-plane into buckling mode. When the pressure increases the surface will crack on the outside of the shell, along the circumferential of the structure.

Figure 9.2: Compression of shell in cut out

To avoid buckling, the structure would need strengthening. An increase of shell thickness would not be an effective option, as it would require a large increase to negate the buckling. The most effective solution are the use of stiffeners, as shown in figure 9.3. The different stiffener options are either longitudinal, circumferential or a combination of both. Stiffeners can have different type of flanges, or no flange, dependent on the purpose. Shell buckling, which is the case here, have shown to be effectively counteracted by use of longitudinal stiffeners [15, ch. 5 p. 5].

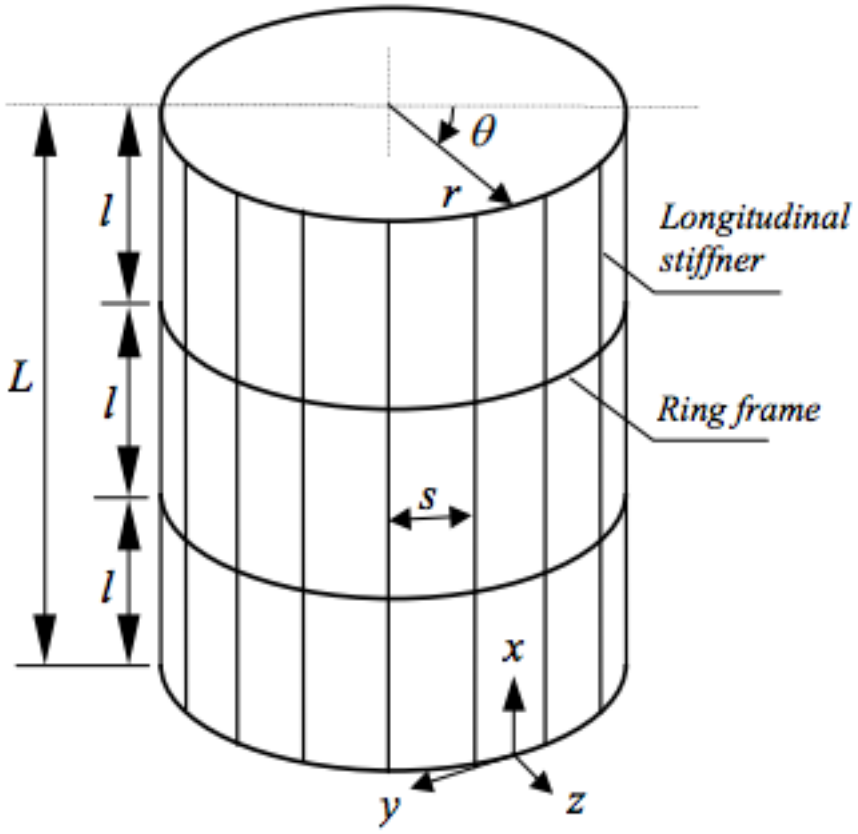

Figure 9.3: Stiffening

For the stiffener to be effective the distance "s" between the stiffeners must not be to large. Longitudinal stiffeners are effective for Batdorf parameter values of Z_s<50 [15, ch. 5 p. 19].

$$Z_s = \frac{s^2}{rt}\sqrt{1-\nu^2} \tag{9.1}$$

Where s is the distance between the longitudinal stiffeners, r is the tower radius, t is the shell thickness and ν is the Poisson´s ratio. This indicates a stiffener spacing of 1m or less for the stiffening to be effective.

As it is mainly in the lower parts of the structure that buckling occur, it might not be necessary with stiffening all the way to the top. It might not even be necessary for stiffening along the entire circumference as it will be the sea-facing side of the tower that has the largest compression, and thus the risk of buckling.

Stiffeners should be added to the structure, and another analysis should be performed, but due to the paper deadline, this will be added to the further work section.

A third option for reducing the problem both with buckling and stress concentrations, as discussed in section 9.3, is to remove the ventilation cut outs from the lower parts of the flare tower. As described in section 8, the cut outs are introduced mainly to reduce vortex induced vibrations. This would primarily be a problem in the upper half of the tower. Removal of the ventilation cut outs from the bottom 10 meters or so could be a fast and effective way of solving these problems.

9.6 Fraction and Fatigue

Due to limited time, no fracture of fatigue considerations have been performed. This is highly important for the life time assessment of the structure, as stated multiple times in different sections. This task has been added to the Further work section.

9.7 Recommendations

Even though there are many subjects remaining before a complete study of the flare tower can be presented, the structure appears to be well dimensioned. The primary calculations show that the tower is strong enough for the loads applied. Aspects like plasticity due to concentration points and buckling might be a problem, but should be able to be accounted for by simple design modifications. A fatigue analysis would show wether the model needs strengthening to give a satisfactory life span.

Other aspects that need to be enlightened are the effect of VIV on the structure, which could have a substantial impact on the structural integrity. In this regard a model test would be recommended.

9.8 Further work

Certain aspects have not been examined, due to a limited amount of time. The known remaining tasks related to the novel flare tower are as follows:

- Longitudinal stiffeners in the lower part of the structure to see if it counteracts the local shell buckling.
- Check wether removal of the lower ventilation cut outs would remove local buckling and stress concentration problems.
- Run a fatigue analysis of the structure with no significant starter cracks, and with large cracks in the ventilation areas due to local buckling, to analyze the structural life span.
- ALS analysis with 10^{-4} annual probability return loads.
- Perform a model test or CFD analysis to examine the effect of the ventilation cut outs on VIV suppression.

Bibliography

[1] NORSOK N-001; *"Structural design"*. Standards Norway, Rev.4, February 2004.

[2] NORSOK N-003; *"Actions and action effects"*. Standards Norway, Edition 2, September 2007.

[3] NORSOK N-004; *"Design of steel structures"*. Standards Norway, Rev.2, October 2004.

[4] NORSOK M-120; *"Material data sheets for structural steel"*. Standards Norway, Rev.4, June 2004.

[5] Eurocode NS-EN 1991-1-4; *"General actions - Wind actions"*. Standards Norway, 2005+NA:2009.

[6] Ivar Langen, Ragnar Sigbjørnsson; *"Dynamisk analyse av kontruksjoner"*. Tapir, 1979.

[7] O.M. Faltinsen; *"Sea loads on ships and offshore structures"*. Cambridge, 1990.

[8] Emil Simiu, Robert H. Scanlan; *"Wind effects on structures"*. Wiley, 1996.

[9] D.J. Cerda Salzman, J. van der Tempel; *"Aerodynamic damping in the design of support structures for offshore wind turbines"*. Delft University of Technology, 2005.

[10] Arne A. Oppen, Arne Kvitrud; *"Wind induced resonant cross flow vibrations on Norwegian offshore flare booms"*. OMAE Volume 1-B, Offshore technology, ASME 1995.

[11] Kjetil Skaugset, *"On the suppression of vortex induced vibrations of circular cylinders by radial water jets"*. IMT-rapport 2003:2, Trondheim 2003.

[12] Torgeir Moan; *"Design of offshore structures"*. Trondheim 2004.

[13] Sverre K. Haver; *"Prediction of characteristic response for design porposes"*. Revision 2, 2009.

[14] Bernt J. Leira; *"Marine konstruksjoner grunnkurs"*. 2009.

[15] Jørgen Amdahl; *"Buckling and ultimate strength of marine structures"*. Trondheim 2010.

[16] Kåre Syvertsen; *Flare memo*, 2011.

[17] Jon Eirik Nøding; *Specialization project*, 2011.

Appendix A

Matlab scripts

A.1 Structure

```
file = fopen('Structure.txt', 'w');

% Create points

r=2.5;
i=1;
x=0;
y=0;
z=0;

fprintf(file,'STRING asm_create_grid_xyz_created_ids[VIRTUAL] \n');

for  a = 1:28
    fprintf(file,'asm_const_grid_xyz( "%i", "[0 0 %i]", "Coord 0",
  asm_create_grid_xyz_created_ids ) \n',i,z);
    th=0;
    for b = 1:13
        i=i+1;
        x=r*cos(th);
        y=r*sin(th);
        fprintf(file,'asm_const_grid_xyz( "%i", "[%i %i %i]", "Coord 0",
  asm_create_grid_xyz_created_ids ) \n',i,x,y,z);
        th=th+pi()/6;
    end

    fprintf(file, '$? YESFORALL 1000034 \n' );

    i=i+1;
    z=z+2;
    r=r-0.05;

end

% Create curves

fprintf(file,'STRING sgm_create_curve_2d_created_ids[VIRTUAL] \n');

i=1;
j=1;
m=1;
n=2;

for a = 1:28
    for b = 1:12
        m=m+1;
```

```
        n=n+1;

        fprintf(file,'sgm_const_curve_2d_arc2point_v2( "%i", 1, 0., FALSE,
 FALSE, 1, "Coord 0.3",  "Point %i", "Point %i", "Point %i", FALSE,
 sgm_create_curve_2d_created_ids ) \n',i,j,m,n);
        i=i+1;
        end
    j=j+14;
    m=j;
    n=j+1;

end

% Create surfaces between curves

fprintf(file,'STRING sgm_surface_2curve_created_ids[VIRTUAL] \n');

i=1;
j=1;
k=13;

for a = 1:27
    for b = 1:12
    fprintf(file,'sgm_const_surface_2curve( "%i", "Curve %i", "Curve %i",
  sgm_surface_2curve_created_ids ) \n', i,j,k);
    i=i+1;
    j=j+1;
    k=k+1;
    end
end

fprintf(file, 'loadsbcs_create2( "BC", "Displacement", "Nodal", "", "Static",
["Point 1:14 Curve 1:12"],
 "Geometry", "Coord 0", "1.", ["< 0 0 0  >", "< 0 0 0  >", "<     >", "<
>"], ["", "", "", ""] ) \n');

fclose(file);
```

A.2 Ventilation

```
file = fopen('Ventilation.txt', 'w');


%Create curves

fprintf(file,'STRING sgm_create_curve_2d_created_ids[VIRTUAL] \n');
fprintf(file,'sgm_const_curve_2d_circle_v2( "401", 1, 0.3, "Coord
0.1", "", "[0 0 1]", FALSE, sgm_create_curve_2d_created_ids ) \n');
fprintf(file,'sgm_const_curve_2d_circle_v2( "402", 1, 0.3, "Coord
0.2", "", "[0 0 1]", FALSE, sgm_create_curve_2d_created_ids ) \n');


%Create surface extrude

fprintf(file,'STRING sgm_sweep_surface_e_created_ids[VIRTUAL]\n');
fprintf(file,'sgm_const_surface_extrude( "401", "<3 0 0>", 1., 0.,
"[0 0 0]","Coord 0", "Curve 401", sgm_sweep_surface_e_created_ids )\n');
fprintf(file,'sgm_const_surface_extrude( "402", "<0 3 0>", 1., 0.,
"[0 0 0]","Coord 0", "Curve 402", sgm_sweep_surface_e_created_ids )\n');
fprintf(file,'sgm_const_surface_extrude( "403", "<-3 0 0>", 1., 0.,
"[0 0 0]","Coord 0", "Curve 401", sgm_sweep_surface_e_created_ids )\n');
fprintf(file,'sgm_const_surface_extrude( "404", "<0 -3 0>", 1., 0.,
"[0 0 0]","Coord 0", "Curve 402", sgm_sweep_surface_e_created_ids )\n');


%Rotate surfaces

fprintf(file,'STRING sgm_transform_surf__created_ids[VIRTUAL] \n');
fprintf(file,'sgm_transform_rotate( "405", "surface", "Coord 0.3",
15., 0.,"Coord 0", 1, TRUE, "Surface 401:404", sgm_transform_surf_
_created_ids ) \n'); fprintf(file,'$? YES 38000219 \n');


%Translate and rotate surfaces

i=409;
j=405;
k=408;
for a=1:9
    for b=1:2

        fprintf(file,'sgm_transform_translate_v1( "%i", "surface",
"<0 0 2>", 2., FALSE, "Coord 0", 1, FALSE, "Surface %i:%i",
 sgm_transform_surf__created_ids ) \n',i,j,k);
```

```
        i=i+4;
        j=j+4;
        k=k+4;

        fprintf(file,'sgm_transform_rotate( "%i", "surface", "Coord 0.3",
 30., 0., "Coord 0", 1, TRUE, "Surface %i:%i",
 sgm_transform_surf__created_ids ) \n',i,j,k);
        fprintf(file,'$? YES 38000219 \n');

        i=i+4;
        j=j+4;
        k=k+4;
    end

    if i<613
        fprintf(file,'sgm_transform_translate_v1( "%i", "surface", "<0 0 2>"
, 2., FALSE, "Coord 0", 1, FALSE, "Surface %i:%i",
sgm_transform_surf__created_ids ) \n',i,j,k);

        i=i+4;
        j=j+4;
        k=k+4;

        fprintf(file,'sgm_transform_rotate( "%i", "surface", "Coord 0.3",
-60., 0., "Coord 0", 1, TRUE, "Surface %i:%i",
sgm_transform_surf__created_ids ) \n',i,j,k);
        fprintf(file,'$? YES 38000219 \n');

        i=i+4;
        j=j+4;
        k=k+4;
    end
end


% Create curves

fprintf(file,'STRING sgm_create_curve_in_created_ids[VIRTUAL] \n');


i=403;
j=1;
k=405;
for a=1:27
    for b=1:3
        if i<508
            for c=1:4
                fprintf(file,'sgm_const_curve_intersect( "%i", 1, "Surface
%i","Surface %i", 0.005, 0.05, sgm_create_curve_in_created_ids ) \n',i,j,k);
```

```
                i=i+1;
                j=j+3;
                k=k+1;
            end
            j=j+1;
            k=k+4;
        end
    end
    j=j-3;
end


% Surface break

fprintf(file,'STRING sgm_surface_break_c_created_ids[VIRTUAL] \n');

i=701;
j=1;
k=403;
for a=1:27
    for b=1:3
        if i<806
            for c=1:4
                fprintf(file,'sgm_edit_surface_break_v1( "%i",
"Surface %i",TRUE, 3, 0, 0., "", "", "Curve %i", sgm_surface_
break_c_created_ids ) \n',i,j,k);
                fprintf(file,'$? YESFORALL 1000035 \n');
                fprintf(file,'$? YES 38000219 \n');
                i=i+1;
                j=j+3;
                k=k+1;
            end
            j=j+1;
        end
    end
    j=j-3;
end

% Surface delete
fprintf(file,'STRING asm_delete_surface_deleted_ids[VIRTUAL] \n');
fprintf(file,'asm_delete_surface( "Surface 405:616",
asm_delete_surface_deleted_ids ) \n');

fclose(file);
```

A.3 Eurocode approximation

```
%Basic wind

C_dir=1.0;
C_season=1.0;
V_b0=32*1.34;
V_b=C_dir*C_season*V_b0;

%Middle wind
k_r=0.16;
z_0=0.003;
C_0=1.0;
for z=16:70
    C_r(z)=k_r*log(z/z_0); % z is considerably larger than z_min
    V_m(z)=C_r(z)*C_0*V_b;
end

%Tubulence intensity
k_I=1.0;
sig_v=k_r*V_b*k_I;
for z=16:70
    I_v(z)=sig_v/V_m(z); % z is considerably larger than z_min
end

%Peak velocity pressure
rho_air=1.25;
for z=16:70
    q_p(z)=(1+7*I_v(z))*.5*rho_air*V_m(z)^2;
end

%Force factor
z_e=52;
b=3.65;
nu_air=1.529*10^-5;
v=sqrt(2*q_p(z_e)/rho_air);
Re=b*v/nu_air;
k=2*10^-5;
% c_f0=0.11/(Re/10^6)^1.4; %for Re smaller than 10^4
c_f0=1.2+(0.18*log10(10*k/b))/(1+0.4*log10(Re/10^6)); %for Re larger than 10^4
psi=0.7;
c_f=c_f0*psi;

%Construction factor c_sc_d
z_s=48;
L_t=300;
z_t=200;
```

```
alph=0.67+0.05*log(z_0);
for z=16:70
    L(z)=L_t*(z/z_t)^alph; % z is considerably larger than z_min
end

h=54.0;
b=3.65;
B2=1/(1+0.9*((b+h)/L(z_s))^0.63);
n_1x=1.43535; %-------Eigenfrequency for mode 1 from Abaqus

for z=16:70
    f_L(z)=n_1x*L(z)/V_m(z);
    S_L(z)=(6.8*f_L(z))/(1+10.2*f_L(z))^(5/3);
end

n_h=4.6*h/L(z_s)*f_L(z_s);
R_h=1/n_h-1/(2*n_h^2)*(1-exp(-2*n_h));
n_b=4.6*b/L(z_s)*f_L(z_s);
R_b=1/n_b-1/(2*n_b^2)*(1-exp(-2*n_b));

t=0.01; % Shell thickness dependent
rho_steel=7.850*10^3;
zeta=2.0;
h=54;

for z=1:54
    mu(z)=pi()*(5-0.05*z)*t*rho_steel;
    phi2(z)=((z/h)^zeta)^2;
    mu_phi(z)=mu(z)*phi2(z);
end

mu_e=trapz(mu_phi)/trapz(phi2);
d_a=(c_f*rho_air*V_m(z_s))/(2*n_1x*mu_e);
d_s=0.012;
d_d=0.0;
d=d_s+d_a+d_d;
R2=pi()^2/2*d*S_L(z_s)*R_h*R_b;
T=600;
nu=n_1x*sqrt(R2/(B2+R2));
k_p=sqrt(2*log(nu*T))+0.6/sqrt(2*log(nu*T));
if k_p>3.0
else
    k_p=3.0;
end
C_sC_d=(1+2*k_p*I_v(z_s)*sqrt(B2+R2))/(1+7*I_v(z_s));

%Wind force

F_w=C_sC_d*c_f*q_p(z_e); %*area
```

A.4 Wind specter

```
file = fopen('Specter.txt', 'w');

rho_air=1.25;
z_e=52;
k_10=0.0025;

U_R=43;
z_r=10;
alpha=0.10;
U=U_R*(z_e/z_r)^alpha;
U_10=U_R*(10/z_r)^alpha;

h=43;
b=3.65;
nu_air=1.529*10^-5;
Re=b*U/nu_air; % => Re=1.2*10^7 + Figure 4.5.5.c => C_Ds=0.7
C_Ds=0.7;
C_D=C_Ds*(1-0.015*(20-h/b));

u_star=sqrt(k_10)*U_10;
a=120; % Number of frequency steps, highest frequency = a*0.05
delta_n=0.05; % Size of each frequency step

for i=1:a

    n(i)=0.05*i; % Gives frequencies with intervals of 0.05 Hz
    f=(n(i)*z_e)/(U);
    S(i)=200*f/(1+50*f^(5/3))*u_star^2/n(i);
    u(i)=sqrt(2*S(i)*delta_n);
    q_t(i)=(0.5*rho_air*C_D*U^2+rho_air*C_D*U*u(i))*1.3;

%     fprintf(file,'%i, %i \n',n(i),1); % To create unit load input
    fprintf(file,'%i, %i \n',n(i),q_t(i));
end % q_t multiplied with 1.3 in accordance with the NORSOK standard

plot(n,q_t);
xlabel('FREQUENCY Hz');
ylabel('PRESSURE Pa');

fclose(file);
```

A.5 Response specter

```
file = fopen('Specter.txt');
spec=fscanf(file,'%f, %f', [2 inf]);
freq=spec(1,:);
pres_spec=spec(2,:);
fclose(file);

% Without damping
resp(1,:)=; % 120 values from Abaqus analysis
% 3% of critical damping
resp(2,:)=; % 120 values from Abaqus analysis
% 5% of critical damping
resp(3,:)=; % 120 values from Abaqus analysis

for j=1:3
    for i=1:120
        resp_spec(j,i)=pres_spec(i)/10^6*resp(j,i)*10^2;
        resp_spec_0(j,i)=0.5*(pres_spec(i)/10^6*resp(j,i)*10^2)^2;
        resp_spec_2(j,i)=0.5*(pres_spec(i)/10^6*resp(j,i)*10^2)^2
*freq(i)^2;
    end
end

figure(1);
plot(freq,resp(:,:)*10^2);
xlabel('FREQUENCY [Hz]');
ylabel('VONMISES RESPONSE [-]');
axis([0 6 0 1.5*10^6]);
legend('No damping','3% Critical damping','5% Critical damping')

figure(2);
plot(freq,resp_spec);
xlabel('FREQUENCY [Hz]');
ylabel('VONMISES RESPONSE [MPa]');
axis([0 6 0 100]);
legend('No damping','3% Critical damping','5% Critical damping')

delta_n=0.05;
m_0=trapz(resp_spec_0(2,:))*delta_n;
m_2=trapz(resp_spec_2(2,:))*delta_n;
sigma=sqrt(m_0); % Standard deviation
t=sqrt(m_0/m_2); % Zero-upcrossing Period
tau=10; % 10 min timesample \cite[p.104]{Eurocode}
n=60*tau/t; % Number of global maxima in 10 min
E_max=sigma*(sqrt(2*log(n))+0.5772/sqrt(2*log(n)));
% E_max is the expected largest value
```

Appendix B

Patran sessions

B.1 Properties

```
material.create( "Analysis code ID", 2, "Analysis type ID", 1,@
"Steel",0, "Date: 30—May—12 Time: 18:21:53", "Isotropic", 1,@
"Directionality",1, "Linearity", 1, "Homogeneous", 0, "Elastic"@
, 1, "Model Options & IDs",["None", "Instantaneous", "", "", ""]@
, [30, 137, 0, 0, 0], "Active Flag",1, "Create", 10, "External@
Flag", FALSE, "Property IDs",["Elastic Modulus","Poisson's Ratio"@
, "Density", "Mass Propornl Damping", "Stiffness Propornl Damping"]@
, [2, 5, 16, 1001, 1002, 0],"Property Values",["205000000000",@
"0.3", "7850", "0.0685", "0.0086", ""] )

elementprops_create( "Thick10", 51, 25, 35, 1, 1, 20, [13, 1080,@
1071,21, 1079, 20, 1279, 1066, 1067, 1068, 1069], [5, 1, 3, 9, 3@
, 1, 1, 1, 1,1, 1], ["m:Steel", "0.01", "", "", "", "", "", "",@
"", "", ""], "Surface2 3 5 6 8 9 11:13 15 16 18 19 21 22 24:26@
28 29 31 32 34 35 38 39 41 42 44 45 47:49 51 52 54 55 57 58 60:62@
64 65 67 68 70 71 74 75 77 78 80 81 83:85 87 88 90 91 93 94 96:98@
100 101 103 104 106 107 110 111 113 114 116 117 119:121 123 124@
126 127 129 130 132:134 136 137 139 140 142 143 146 147 149 150@
152 153 155:157 159 160 162 163 165 166 168:170 172 173 175 176@
178 179 182 183 185 186 188 189 191:193 195 196 198 199 201 202@
204:206 208 209 211 212 214 215 218 219 221 222 224 225 227:229@
231 232 234 235237 238 240:242 244 245 247 248 250 251 254 255@
257 258 260 261 263:265 267 268 270 271 273 274 276:278 280 281@
283 284 286 287 290 291 293 294 296 297 299:301 303 304 306 307@
309 310 312:314 316 317 319 320 322 323 701:809" )

loadsbcs_create2( "BC", "Displacement", "Nodal", "", "Static",@
["Point 1:14 Curve 1:12"], "Geometry", "Coord 0", "1.", ["< 0@
0 0  >", "< 0 0 0 >", "<  >", "<     >"], ["", "", "", ""] )

elementprops_create( "Pipe_ladder", 1, 25, 18, 27, 2, 15, [1010@
, 1011, 1012], [1, 1, 1], ["308", "", ""], "Point 16:366:14" )
elementprops_create( "Flare_pack", 1, 25, 18, 27, 2, 15, [1010,@
1011, 1012], [1, 1, 1], ["208", "", ""], "Point 380:391" )

STRING fem_create_elemen_elems_created[VIRTUAL]
fem_create_elems_1( "Point ", "Point", "1", "Standard", 3,@
"Point 380:391", "" , "", "", "", "", "", "",@
fem_create_elemen_elems_created )
fem_associate_elems_to_ep( "Flare_pack", "1:12", 1 )
fem_create_elems_1( "Point ", "Point", "13", "Standard", 3,@
"Point 16:366:14", "", "", "", "", "", "", "",@
fem_create_elemen_elems_created )
fem_associate_elems_to_ep( "Pipe_ladder", "13:38", 1 )
```

B.2 Meshing

```
INTEGER fem_create_mesh_surfa_num_nodes
INTEGER fem_create_mesh_surfa_num_elems
STRING fem_create_mesh_s_nodes_created[VIRTUAL]
STRING fem_create_mesh_s_elems_created[VIRTUAL]
fem_create_mesh_surf_4( "Hybrid", 49680, "Surface 2 3 5 6 8 9 11:13@
15 16 18 19 21 22 24:26 28 29 31 32 34 35 38 39 41 42 44 45 47:49@
51 52 54 55 57 58 60:62 64 65 67 68 70 71 74 75 77 78 80 81 83:85@
87 88 90 91 93 94 96:98 100 101 103 104 106 107 110 111 113 114 116@
117 119:121 123 124 126 127 129 130 132:134 136 137 139 140 142 143@
146 147 149 150 152 153 155:157 159 160 162 163 165 166 168:170 172@
173 175 176 178 179 182 183 185 186 188 189 191:193 195 196 198 199@
201 202 204:206 208 209 211 212 214 215 218 219 221 222 224 225@
227:229 231 232 234 235 237 238 240:242 244 245 247 248 250 251 254@
255 257 258 260 261 263:265 267 268 270 271 273 274 276:278 280 281@
283 284 286 287 290 291 293 294 296 297 299:301 303 304 306 307 309@
310 312:314 316 317 319 320 322 323 701:809", 4, ["0.2", "0.1",@
"0.2", "1.0"], "Tria3" , "#","#", "Coord 0", "Coord 0",@
fem_create_mesh_surfa_num_nodes, fem_create_mesh_surfa_num_elems,@
fem_create_mesh_s_nodes_created, fem_create_mesh_s_elems_created )

REAL fem_equiv_all_x_equivtol_ab

INTEGER fem_equiv_all_x_segment

fem_equiv_all_group4( [" "], 0, "", 1, 1, 0.01, FALSE, @
fem_equiv_all_x_equivtol_ab, fem_equiv_all_x_segment )
```

B.3 Eurocode wind load

```
loadcase_create2( "Static", "Static", "", 1., ["BC"], [0], [1.], "",@
0., TRUE )

loadsbcs_create2( "Acc_gen", "Inertial Load", "Element Uniform",@
"2D", "Static", ["Surface 2 3 5 6 8 9 11:13 15 16 18 19 21 22 24:26@
28 29 31 32 34 35 38 39 41 42 44 45 47:49 51 52 54 55 57 58 60:62 64@
65 67 68 70 71 74 75 77 78 80 81 83:85 87 88 90 91 93 94 96:98 100@
101 103 104 106 107 110 111 113 114 116 117 119:121 123 124 126 127@
129 130 132:134 136 137 139 140 142 143 146 147 149 150 152 153@
155:157 159 160 162 163 165 166 168:170 172 173 175 176 178 179 182@
183 185 186 188 189 191:193 195 196 198 199 201 202 204:206 208 209@
211 212 214 215 218 219 221 222 224 225 227:229 231 232 234 235 237@
238 240:242 244 245 247 248 250 251 254 255 257 258 260 261 263:265@
267 268 270 271 273 274 276:278 280 281 283 284 286 287 290 291 293@
294 296 297 299:301 303 304 306 307 309 310 312:314 316 317 319 320@
322 323 701:809"], "Geometry", "Coord 0", "1.",@
["<4.75 0 −12.15>","<     >", "<     >"], ["", "", ""] )

loadsbcs_create2( "Acc_add", "Inertial Load", "Element Uniform",@
"0D", "Static", ["Element 1:38"], "FEM", "Coord 0", "1.", ["<4.75@
0 −12.15>", "<     >", "<     >"], ["", "", ""] )

loadsbcs_create2( "Pres", "Pressure", "Element Uniform", "2D",@
"Static", [ "Surface 5 6 8 9 16 18 19 21 28 29 31 32 41 42 44 45@
52 54 55 57 64 65 67 68 77 78 80 81 88 90 91 93 100 101 103 104 113@
114 116 117 124 126 127 129 136 137 139 140 149 150 152 153 160 162@
163 165 172 173 175 176 185 186 188 189 196 198 199 201 208 209 211@
212 221 222 224 225 232 234 235 237 244 245 247 248 257 258 260 261@
268 270 271 273 280 281 283 284 293 294 296 297 304 306 307 309 316@
317 319 320 702 703 706 707 710 711 714 715 718 719 722 723 726 727@
730 731 734 735 738 739 742 743 746 747 750 751 754 755 758 759 762@
763 766 767 770 771 774 775 778 779 782 783 786 787 790 791 794 795@
798 799 802 803 806 807"], "Geometry", "", "1.", ["2688 ", " ", " "]@
, ["", "", ""] )
```

B.4 Wind specter load

```
loadcase_create2( "Freq", "Time Dependent", "", 1., ["BC"], [0],@
[1.] , "", 0., TRUE )

fields_create( "Freq", "Non-Spatial", 1, "Scalar", "Real", "",@
"", "Table", 1, "f", "", "", "", "", "", FALSE, [0.050000001,@
0.1, 0.15000001, 0.2, 0.25, 0.30000001, 0.34999999, 0.40000001,@
0.44999999, 0.5, 0.55000001, 0.60000002, 0.64999998, 0.69999999,@
0.75, 0.80000001, 0.85000002, 0.89999998, 0.94999999, 1., 1.05,@
1.1, 1.15, 1.2, 1.25, 1.3, 1.35, 1.4, 1.45, 1.5, 1.55, 1.6, 1.65,@
1.7, 1.75, 1.8, 1.85, 1.9, 1.95, 2., 2.05, 2.0999999, 2.1500001,@
2.2, 2.25, 2.3, 2.3499999, 2.4000001, 2.45, 2.5, 2.55, 2.5999999,@
2.6500001, 2.7, 2.75, 2.8, 2.8499999, 2.9000001, 2.95, 3., 3.05,@
3.0999999, 3.1500001, 3.2, 3.25, 3.3, 3.3499999, 3.4000001, 3.45,@
3.5, 3.55, 3.5999999, 3.6500001, 3.7, 3.75, 3.8, 3.8499999,@
3.9000001, 3.95, 4., 4.0500002, 4.0999999, 4.1500001, 4.1999998,@
4.25, 4.3000002, 4.3499999, 4.4000001, 4.4499998, 4.5, 4.5500002@
 4.5999999, 4.6500001, 4.6999998, 4.75, 4.8000002, 4.8499999,@
4.9000001, 4.9499998, 5., 5.0500002, 5.0999999, 5.1500001,@
5.1999998, 5.25, 5.3000002, 5.3499999, 5.4000001, 5.4499998, 5.5,@
5.5500002, 5.5999999, 5.6500001, 5.6999998, 5.75, 5.8000002,@
5.8499999, 5.9000001, 5.9499998, 6.], [0.], [0.], @
[[[1.]][[1.]][[1.]][[1.]][[1.]][[1.]][[1.]][[1.]][[1.]][[1.]][[1.]]@
[[1.]][[1.]][[1.]][[1.]][[1.]][[1.]][[1.]][[1.]][[1.]][[1.]][[1.]]@
[[1.]][[1.]][[1.]][[1.]][[1.]][[1.]][[1.]][[1.]][[1.]][[1.]][[1.]]@
[[1.]][[1.]][[1.]][[1.]][[1.]][[1.]][[1.]][[1.]][[1.]][[1.]][[1.]]@
[[1.]][[1.]][[1.]][[1.]][[1.]][[1.]][[1.]][[1.]][[1.]][[1.]][[1.]]@
[[1.]][[1.]][[1.]][[1.]][[1.]][[1.]][[1.]][[1.]][[1.]][[1.]][[1.]]@
[[1.]][[1.]][[1.]][[1.]][[1.]][[1.]][[1.]][[1.]][[1.]][[1.]][[1.]]@
[[1.]][[1.]][[1.]][[1.]][[1.]][[1.]][[1.]][[1.]][[1.]][[1.]][[1.]]@
[[1.]][[1.]][[1.]][[1.]][[1.]][[1.]][[1.]][[1.]][[1.]][[1.]][[1.]]@
[[1.]][[1.]][[1.]][[1.]][[1.]][[1.]][[1.]][[1.]][[1.]][[1.]][[1.]]@
[[1.]][[1.]][[1.]][[1.]][[1.]][[1.]][[1.]][[1.]][[1.]][[1.]]])

loadsbcs_create2( "Freq", "Pressure", "Element Uniform", "2D",@
"Time Dependent", ["Surface 5 6 8 9 16 18 19 21 28 29 31 32 41 42@
44 45 52 54 55 57 64 65 67 68 77 78 80 81 88 90 91 93 100 101 103@
104 113 114 116 117 124 126 127 129 136 137 139 140 149 150 152@
153 160 162 163 165 172 173 175 176 185 186 188 189 196 198 199@
201 208 209 211 212 221 222 224 225 232 234 235 237 244 245 247@
248 257 258 260 261 268 270 271 273 280 281 283 284 293 294 296@
297 304 306 307 309 316 317 319 320 702 703 706 707 710 711 714@
715 718 719 722 723 726 727 730 731 734 735 738 739 742 743 746@
747 750 751 754 755 758 759 762 763 766 767 770 771 774 775 778@
779 782 783 786 787 790 791 794 795 798 799 802 803 806 807"],@
"Geometry", "", "1.", [" 1", " ", " "], ["f:Freq", " ", " "] )
```

Appendix C

Platform response

C.1 Heave acceleration

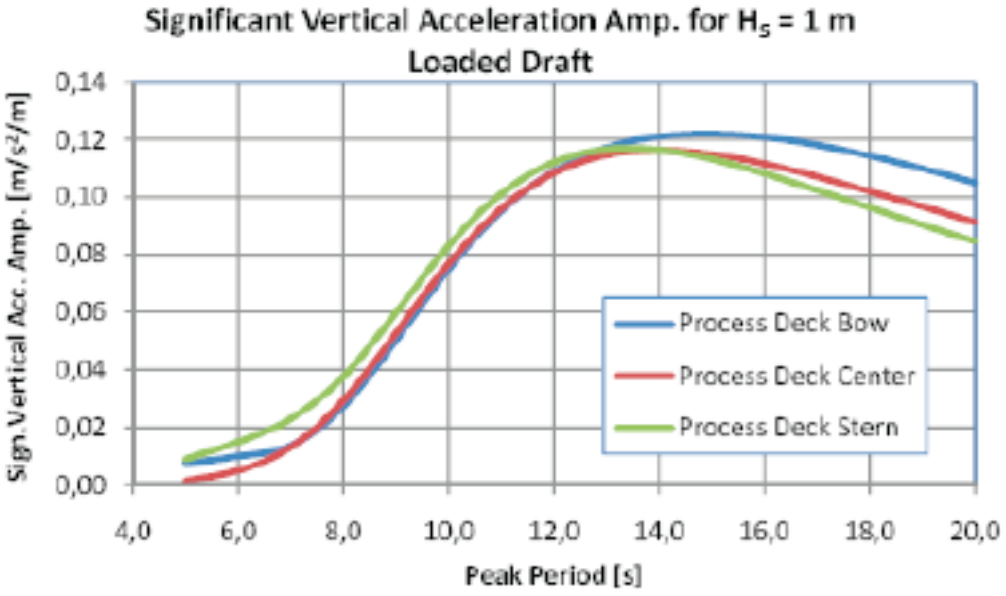

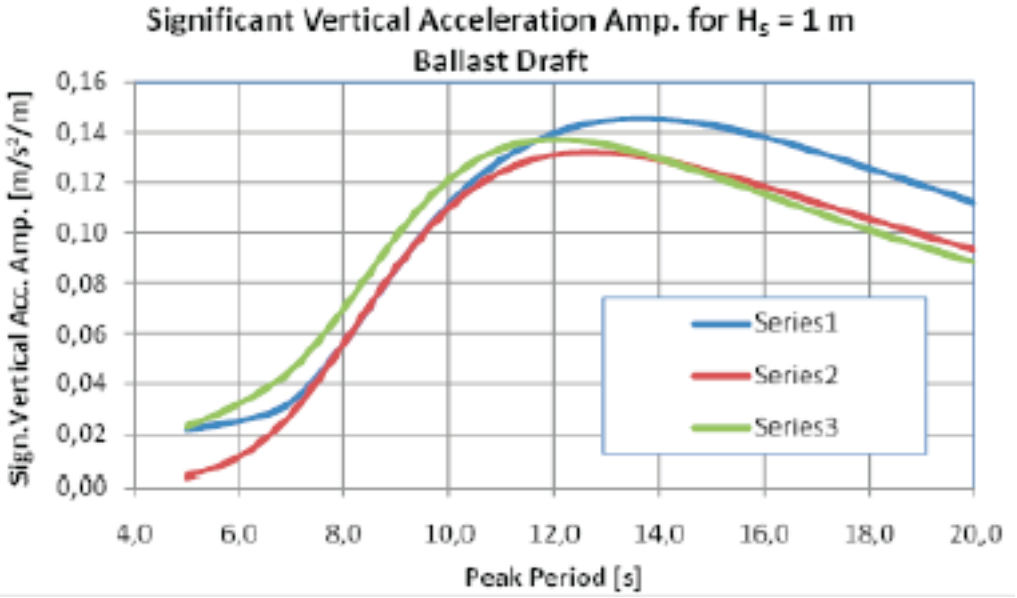

C.2 Surge acceleration